RESIDUAL STRESSES AND DEFLECTIONS DUE TO CLAMPING IN INDETERMINATE STRUCTURES

A THESIS

Presented to

the Faculty of the Graduate Division

by

George Walter Martin

In Partial Fulfillment

of the Requirements for the Degree

Master of Science in Aeronautical Engineering

Georgia Institute of Technology

June, 1958

"In presenting the dissertation as a partial fulfillment of the requirements for an advanced degree from the Georgia Institute of Technology, I agree that the Library of the Institution shall make it available for inspection and circulation in accordance with its regulations governing materials of this type. I agree that permission to copy from, or to publish from, this dissertation may be granted by the professor under whose direction it was written, or, in his absence, by the dean of the Graduate Division when such copying or publication is solely for scholarly purposes and does not involve potential financial gain. It is understood that any copying from, or publication of, this dissertation which involves potential financial gain will not be allowed without written permission.

_____

38
12T

RESIDUAL STRESSES AND DEFLECTIONS DUE TO CLAMPING IN INDETERMINATE STRUCTURES

Approved:

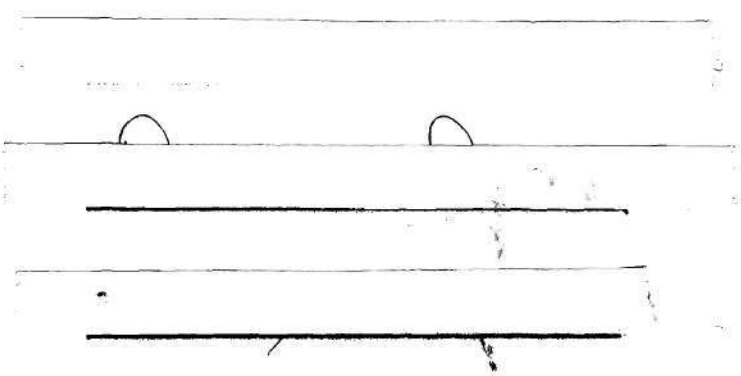

Date Approved by Chairman 6 Sept. 1958

ACKNOWLEDGMENTS

The author wishes to thank Mr. Walter R. Carnes for his assistance during the course of this investigation. Thanks are also extended to Mr. Joseph Neudecker of Lockheed Aircraft Corporation for the thesis topic and to Professor Donnell W. Dutton and Dr. R. Kenneth Jacobs for their critical review of this thesis.

My appreciation is extended to the staff of the Civil Engineering Department and to the personnel of the Aeronautical Engineering Shop and the Mechanical Engineering Foundry for their aid.

TABLE OF CONTENTS

LIST OF TABLES

LIST OF FIGURES

LIST OF SYMBOLS

A	cross sectional area, square inches
b_1, b_2, b_3	bases, inches
c	slope of a rotated face in reference to its original position
c_k	rotation of face K-K, degrees or radians
dA	differential of cross sectional area, square inches
E	modulus of elasticity, pounds per square inch
f_b	bending stress, pounds per square inch
M	moment, inch pounds
P	applied load, pounds
r	radial distance measured outward from the concave side, inches
r_1	distance of the neutral axis from the concave side
R	radius of curvatures of the concave side, inches
t_1, t_2, t_3	radial heights, inches
ϵ	unit strain, inches per inch
δ	elongation of fiber length, inches
δ_K	deflection of point K, inches
δ_i	deflection under the applied load, inches
θ	angular measure, degree or radians
θ_1	lower limit of integration for a segment of constant cross section

ABSTRACT

In many design problems, parts are required that fit onto shafts in such a way that all the play is eliminated between the part and the shaft. It is possible to eliminate this play by clamping the part to the shaft. This method introduces residual stresses and deflections which are difficult to determine analytically since the actual clamping force required depends on the configuration of the part. An approximate analytical solution is presented in this thesis for determining these stresses and deflections as functions of the clamping load and the cross sectional properties of the clamped part.

The deflections, stresses, and clamping load required are determined by the method of strain energy under the simplifying assumption that the strain energy due to bending is the only form of strain energy that needs to be considered. Equations are included that relate the strain energy present to the bending moment applied for rectangular, T-shaped, and I-shaped cross sections.

Two cast bell cranks are used in the experimental part of this thesis to check the validity of this analytical solution. Strain gauges were mounted in several locations in each bell crank to determine the stresses due to clamping, and the deflections were measured by means of a Riehle Extensometer.

The experimental results show an average variation of less than ten per cent as compared to the theoretical results in both the measured stresses and deflections. This shows good correlation between theory and

experiment for the two parts used.

Both the theoretical and experimental parts of this thesis point out that emphasis should be placed on designing clamped parts to be as flexible as possible to decrease the residual stresses obtained from clamping. It is recommended also that several other experimental tests be made on parts of varying cross section and plan form to check the applicability of this method to parts of arbitrary shape.

CHAPTER I

INTRODUCTION

In many design problems, it is necessary to have parts that fit onto shafts in such a way that all the play is eliminated between the part and the shaft. There are several methods that can be used to eliminate this play, one of which is clamping. This involves cutting the part on one side and then forcing the part to fit the shaft by clamping the cut edges together. This method is illustrated below:

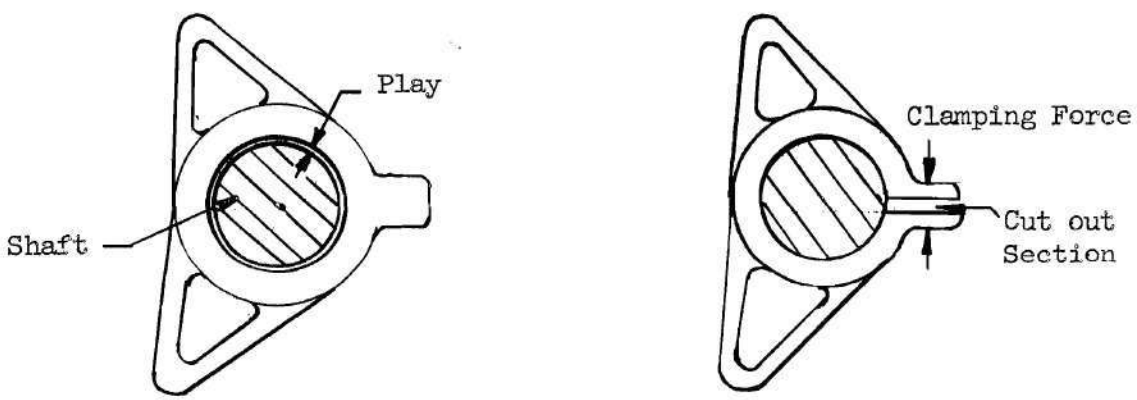

Fig. 1

Clamping Method

The clamping force introduces residual stresses since this clamping force preloads the structure. The author encountered this problem in several of the component parts of a rudder control system. The clamped parts were used to transmit the rudder pedal loads from the pilot to the rudder

actuators. It was necessary to design the parts so that the clamping load would not stress the material beyond the yield stress to satisfy the requirements of the Civil Aeronautics Administration.

The problem was to determine the clamping load needed to decrease the interior diameter a specified amount to ensure a proper fit between the part and the shaft. This involved an indeterminate analysis. The indeterminacy was aggravated, in this case by the variation of the cross sections in the clamped parts and the fact that the depth of the cross section was of the same order of magnitude as the radius of curvature.

An approximate solution to this problem is presented in this thesis. This approximate solution was made by dividing the clamped parts into segments over which the cross sectional properties are assumed to be constant. Several other simplifying assumptions were made in the derivation of the equations in this thesis. These assumptions are discussed in Chapter III.

CHAPTER II

INSTRUMENTATION AND EQUIPMENT

Aluminum Castings.--Two bell cranks were cast with dimensions as shown in Fig. 9, p. 22, and Fig. 13, p. 29. The values of E, the modulus of elasticity, and the yield stress were the only physical properties of the material that were required and they were determined by test (Fig. 8, p. 21).

Tensile Test Bars.--Two cylindrical bars were cast from the same material as the bell cranks and these bars were used to determine the modulus of elasticity, E, and the yield stress. They were machined to the standard A. S. T. dimensions as follows:

1. gauge length - 2 inches
2. diameter along gauge length - 0.50 inches

The test bars were mounted in a Tinius-Olsen Tensile Testing Machine and a plot was obtained of load versus strain.

Tinius-Olsen Tensile Testing Machine.--This machine is constructed so that a plot of load versus strain can be plotted while the actual test is being performed. An electronic strain gauge, the Atcotran - type 6, is connected to the part being tested and is linked electrically to the Olsen Recorder which automatically cross plots a graph of load versus deflection. This Recorder contains a drum on which graph paper is attached; an inking head is then applied to the paper. The electronic strain gauge causes the inking head to move longitudinally along the graph paper, while

the applied load causes the drum to rotate. The plot of load versus strain is then plotted automatically.

Compression Stand.--In the experiments with the deflection of the bell cranks under load, a jig was designed that would simultaneously hold the bell crank in a fixed position and apply the clamping load as a point load to eliminate the possibility of introducing torsional loads. This stand is shown in Fig. 2, p. 5.

Riehle Extensometer and Extensometer Mount.--The deflections were measured with a Riehle Extensometer which was mounted on the bell cranks by means of the Extensometer Mount as shown in Fig. 4, p. 6. The Extensometer Mount is shown in Fig. 3, p. 5.

The scale of the Extensometer is graduated in increments of 0.0002 inches. The measured deflections of the bell cranks varied between 0.003 and 0.014 inches which shows that the graduated scale was in small enough increments to yield accurate readings.

SR-4 Strain Gauges and SR-4 Strain Gauge Indicator.--The stresses were determined with SR-4, AD-7 strain gauges in conjunction with an SR-4 strain gauge indicator. The method used was the standard one for measuring stresses and for this reason no detailed explanation is included. This standard method can be found in Ref. 1.

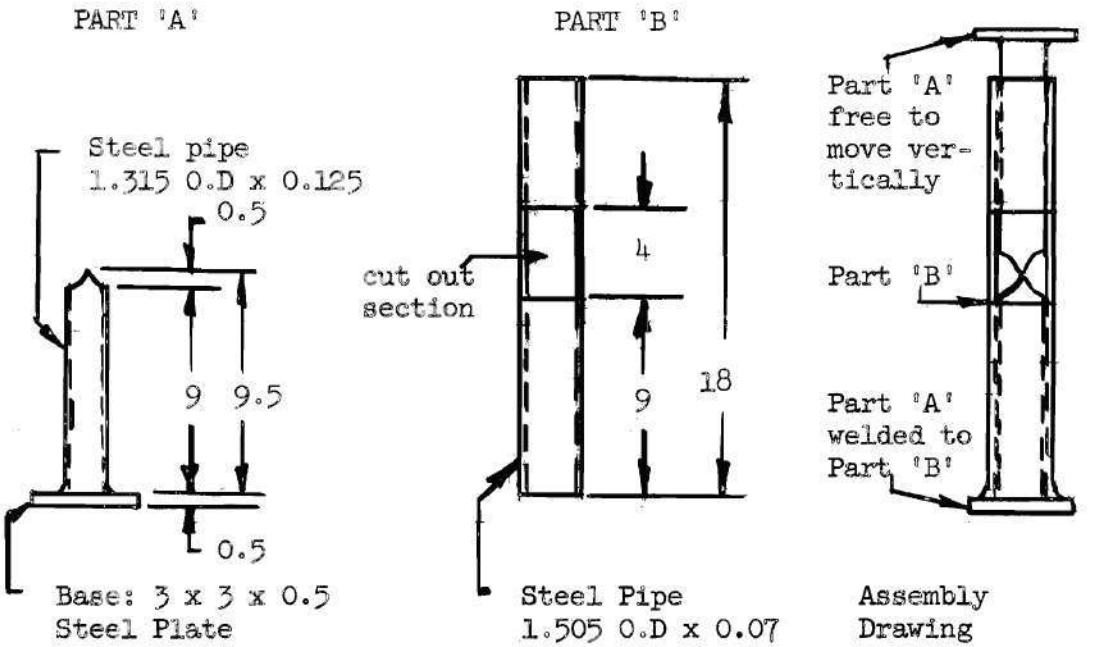

Fig. 2 Compression Stand

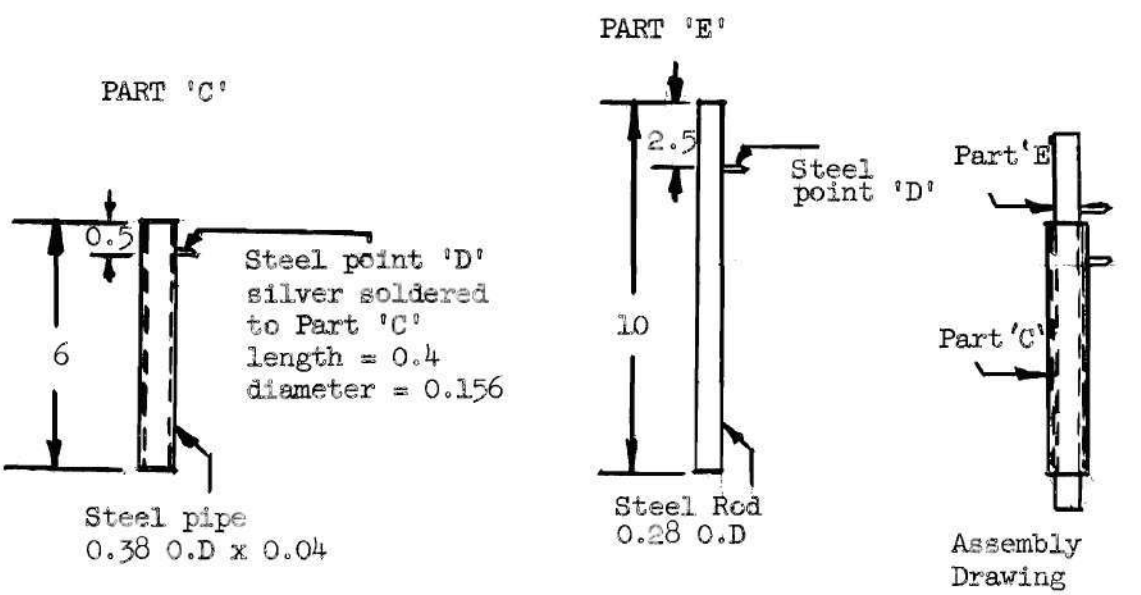

Fig. 3 Extensometer Mount

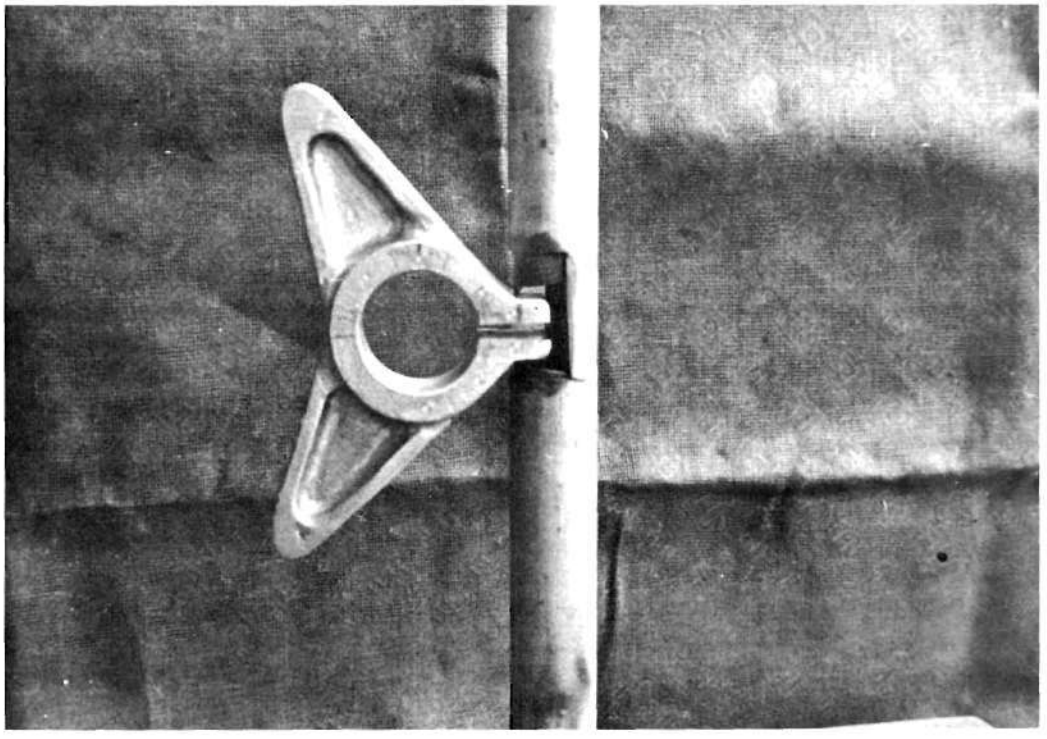

Figure 4. Bell Crank Under Load.

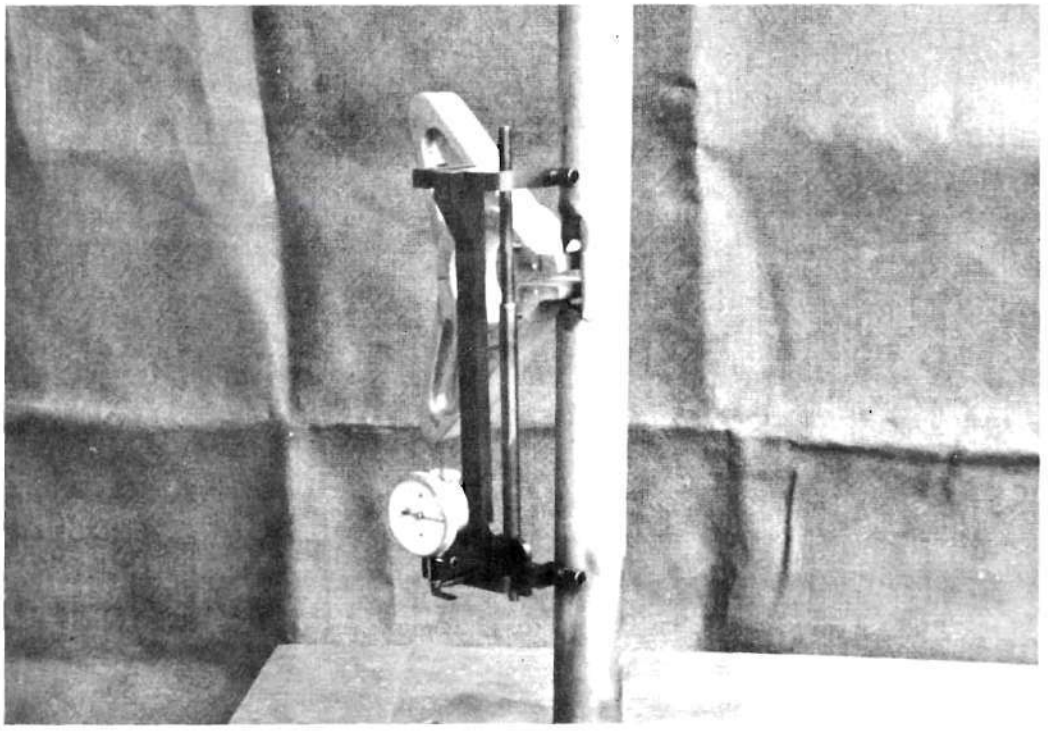

Figure 5. Riehle Extensometer and Extensometer Mount Mounted on Bell Crank.

CHAPTER III

PROCEDURE

Assumptions and Notation.--The methods of strain energy are used in this analysis in which the internal strain energy will be equated to the external energy obtained from the clamping force. Strain energy can be produced in several forms, such as bending, shear, or compression. In order to simplify the equations to be derived the assumption is made that the strain energy due to bending is much greater than the strain energy stored in all other forms. To calculate the amount of strain energy present due to bending, it is necessary to obtain equations relating the amount of rotation of each incremental segment of the part to the bending moment applied to the segment.

The following assumptions are made in the analysis of this rotation:

1. Plane sections remain plane during bending.

2. The only stresses considered are those due to bending.

3. The bell cranks are considered to have constant cross sectional properties over selected segments (see Fig. 6, p. 8, and Fig. 10, p. 23).

4. Displacements and rotations are linear functions of the applied clamping loads.

Three types of cross sections are encountered in this analysis: rectangular, T-shaped, and I-shaped. The equations are derived for an I-shaped cross section and then adapted to the rectangular and T-shaped cross sections.

There are two equations of equilibrium, in conjunction with the assumptions previously stated, that can be used to locate the neutral axis of the section and to establish a relationship between the rotation of a segment to the moment applied. The two equations of equilibrium are:

$$(a) \qquad \int_A f_b \, d\,A = 0$$

$$(b) \qquad \int_A f_b \, y \, d\,A = M$$

Equation (a) specifies that the sum of the forces normal to the surface under consideration is equal to zero, while (b) equates the moment of these forces to the applied moment.

Figure 6 presents the physical dimensions of the I-shaped segment to be analyzed and the notation used in the derivation of the equations.

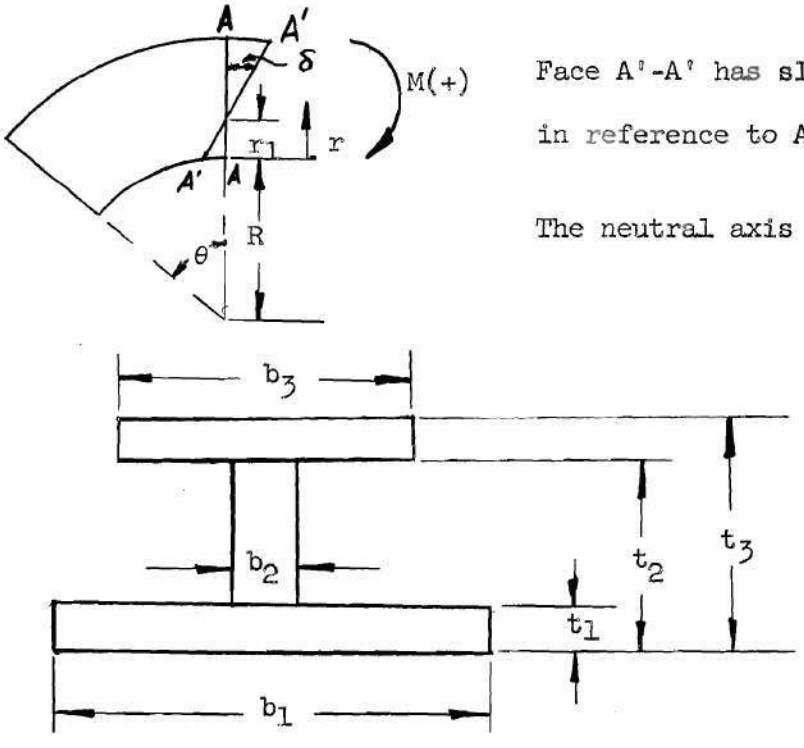

Face A'-A' has slope "c" in reference to A-A.

The neutral axis is located at $r = r_1$.

Fig. 6 Dimensions and Notation

Derivation of Equations.--Under the assumption that plane sections remain plane during bending, face A-A will rotate to A'-A' and the change in length, δ , of any fiber can be expressed as $\delta = c\ (r - r_1)$. The original fiber length is $(R + r)\ \theta$. The value for ϵ can now be obtained by dividing the change in length of any fiber by its original length.

$$\epsilon = \frac{\delta}{(R + r)\ \theta} = \frac{c\ (r - r_1)}{(R + r)\ \theta} \tag{1}$$

Since $f_b = \epsilon\ E$, the bending stress can be evaluated in terms of the rotation of face A-A.

$$f_b = \epsilon\ E = \frac{c\ (r - r_1)}{(R + r)\ \theta} E \tag{2}$$

Equation (a) can now be used to locate the position of the neutral axis which is at $r = r_1$.

$$\int_A f\ d\ A = \int_A \frac{c\ (r - r_1)}{(R + r)\ \theta} E\ d\ A = 0 \tag{3}$$

This integral must be broken up into three integrals due to the discontinuities in the widths, b, at $r = t_1$ and $r = t_2$.

$$\int_A \frac{c\ (r - r_1)}{(R + r)\ \theta} E\ d\ A = \frac{C\ E\ b_1}{\theta} \int_o^{t_1} \frac{r - r_1}{R + r}\ dr + \frac{C\ E\ b_2}{\theta} \int_{t_1}^{t_2} \frac{r - r_1}{R + r}\ dr \tag{4}$$

$$+ \frac{C\,E\,b_3}{\theta} \int_{t_2}^{t_3} \frac{r - r_1}{R + 1}\, dr$$

$$= \frac{C\,E}{\theta} \left\{ b_1 \left[(R + r) - R \ln (R + r) - r_1 \ln (R + r) \right] \Big|_{o}^{t_1} \right.$$

$$+ b_2 \left[(R + r) - R \ln (R + r) - r_1 \ln (R + r) \right] \Big|_{t_1}^{t_2}$$

$$\left. + b_3 \left[(R + r) - R \ln (R + r) - r_1 \ln (R + r) \right] \Big|_{t_2}^{t_3} \right\}$$

$$= 0$$

When the limits have been substituted the equation becomes:

$$\int_A f\, d\, A = b_1 \left[t_1 - R \ln \frac{R + t_1}{R} - r_1 \ln \frac{R + t_1}{R} \right] \qquad (5)$$

$$+ b_2 \left[(t_2 - t_1) - R \ln \frac{R + t_2}{R + t_1} - r_1 \ln \frac{R + t_2}{R + t_1} \right]$$

$$+ b_3 \left[(t_3 - t_2) - R \ln \frac{R + t_3}{R + t_2} - r \ln \frac{R + t_3}{R + t_2} \right]$$

$$= 0$$

This equation can be solved for r_1.

$$r_1 = \frac{b_1\left[t_1 - R\ln\frac{R+t_1}{R}\right] + b_2\left[(t_2 - t_1) - R\ln\frac{R+t_2}{R+t_1}\right]}{b_1\ln\frac{R+t_1}{R} + b_2\ln\frac{R+t_2}{R+t_1} + b_3\ln\frac{R+t_3}{R+t_2}} \tag{6}$$

$$+ \frac{b_3\left[(t_3 - t_2) - R\ln\frac{R+t_3}{R+t_2}\right]}{b_1\ln\frac{R+t_1}{R} + b_2\ln\frac{R+t_2}{R+t_1} + b_3\ln\frac{R+t_3}{R+t_2}}$$

Since $b_1 t_1 + b_2 (t_2 - t_1) + b_3 (t_3 - t_2) = \text{Area}$, the equation for r_1 can be reduced to the form:

$$r_1 = \frac{\text{Area}}{b_1\ln\frac{R+t_1}{R} + b_2\ln\frac{R+t_2}{R+t_1} + b_3\ln\frac{R+t_3}{R+t_2}} - R \tag{7}$$

Equation (b) can now be used, with the moment taken about the neutral axis. The moment arm, since it is measured from r_1, is $(r - r_1)$.

$$\text{Moment} = \int_A \frac{c\,(r - r_1)^2}{(R + r)\,\theta}\,dA \tag{8}$$

$$= \frac{b_1\,C\,E}{\theta}\int_0^{t_1}\frac{(r - r_1)^2}{R + r}\,dr$$

$$+ \frac{b_2\,C\,E}{\theta}\int_{t_1}^{t_2}\frac{(r - r_1)^2}{R + r}\,dr$$

$$+ \frac{b_3 C E}{\theta} \int_{t_2}^{t_3} \frac{(r - r_1)^2}{R + r} \, dr$$

After these integrals have been evaluated the equation for the moment is:

$$\text{Moment} = \frac{C E}{\theta} \left[b_1 A + b_2 B + b_3 D \right] \tag{9}$$

$$A = \left[\frac{(R + t_1)^2}{2} - \frac{R^2}{2} - 2 R t_1 + (R + r_1)^2 \ln \frac{R + t_1}{R} - 2 r_1 t_1 \right] \tag{10-a}$$

$$B = \left[\frac{(R + t_2)^2}{2} - \frac{(R + t_1)^2}{2} + 2 (R + r_1)(t_1 - t_2) + (R + r_1)^2 \ln \frac{R + t_2}{R + t_1} \right] \tag{10-b}$$

$$D = \left[\frac{(R + t_3)^2}{2} - \frac{(R + t_2)^2}{2} + 2 (R + r_1)(t_2 - t_3) + (R + r_1)^2 \ln \frac{R + t_3}{R + t_2} \right] \tag{10-c}$$

The rotation can now be expressed as a function of θ.

$$C = \frac{\text{Moment } \theta}{E \left[b_1 A + b_2 B + b_3 D \right]} \tag{11}$$

If a T-section is used, these equations can be adapted to the T-section by setting one of the bases equal to zero. If a rectangular section is used, two of the bases can be set equal to zero.

In the case of the rectangle, assume b_2 and b_3 are zero. A solution can then be obtained for r_1 and c.

$$r_1 = \frac{\text{Area}}{b_1 \ln \frac{R + t_1}{R}} - R = \frac{b_1 t_1}{b_1 \ln \frac{R + t_1}{R}} - R \qquad (12\text{-a})$$

$$= \frac{t_1 - R \ln \frac{R + t_1}{R}}{\ln \frac{R + t_1}{R}}$$

$$A = \left[\frac{(R + t_1)^2}{2} - \frac{R^2}{2} - 2 R t_1 + (R + r)^2 \ln \frac{R + t_1}{R} \right. \qquad (12\text{-b})$$

$$\left. - 2 r_1 t_1 \right]$$

$$= \left[t_1^2 \left\{ \frac{1}{2} - \frac{1}{\ln \frac{R + t_1}{R}} \right\} + R t_1 \right]$$

$$C = \frac{\text{Moment } \theta}{E \left[b_1 \left\{ t_1^2 \left[\frac{1}{2} - \frac{1}{\ln \frac{R + t_1}{R}} \right] + R t_1 \right\} \right]} \qquad (12\text{-c})$$

A means is now available to equate the strain energy from bending to that of the external energy of the clamping force. The strain energy in any segment of constant cross section can be expressed in integral form.

$$\text{Strain energy} = \int_{\theta_1}^{\theta_2} \frac{\text{Moment } (d\ C)}{2} = \int_{\theta_1}^{\theta_2} \frac{(\text{Moment})^2\ d\ \theta}{2\ E\ \left[b_1\ A + b_2\ B + b_3\ D\right]} \quad (13)$$

θ_1 and θ_2 represent the angular limits of the segment under consideration.

The strain energy can be represented in integral form because the variables, moment and c, are continuous functions of θ on the range $\theta_2 \leq \theta \leq \theta_1$.

The total strain energy from bending is the sum of the strain energies in the segments. The strain energy from the applied load is $\frac{P\ \delta_i}{2}$, where δ_i represents the deflection of the point under the applied load.

$$\frac{P\ \delta_i}{2} = \sum_{j=1}^{n} \left(\int_{\theta_1}^{\theta_2} \frac{(\text{Moment})^2\ d\ \theta}{2\ E\ \ b_1\ A + b_2\ B + b_3\ D} \right)_j \quad (14)$$

(n is the total number of segments)

In the analysis of symmetrical structures, only one-half of the structure need be considered. In this case one end of the structure is considered to be built in. The deflections calculated will be only one-half of the total deflections. Both parts analyzed in this thesis are symmetrical and have been analyzed in this manner.

The deflection of any other point in the structure can be evaluated by transferring the applied load to the point under consideration, with a moment that will put the face at that point in static equilibrium. The strain energies can again be equated.

$$\frac{M\, c_k}{2} + \frac{P\, \delta_k}{2} = \sum_{j=k}^{n} \left(\int_{\theta_1}^{\theta_2} \frac{(\text{Moment})^2\, d\theta}{2\, E\, b\, A + b\, B + b\, D} \right)_j \qquad (15)$$

The summation will start at the point where the deflection is required (this point is represented by k in the summation).

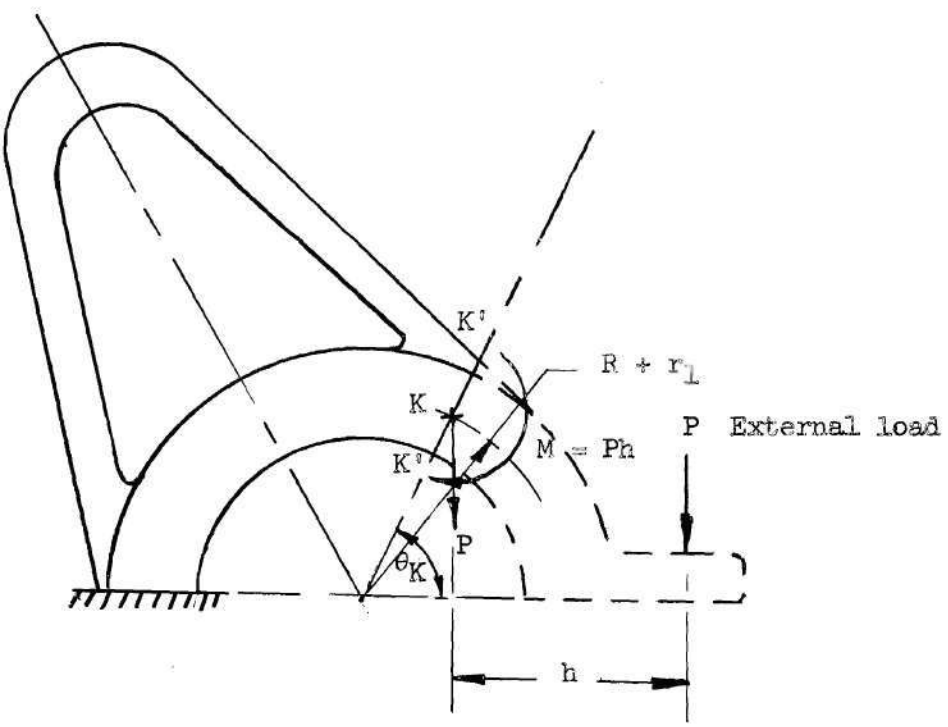

Fig. 7 Internal Loadings

The total external strain energy at K'-K' will be $\frac{P\delta_k}{2} + \frac{M c_k}{2}$, where δ_k represents the vertical deflection of K'-K' and c_k represents the strain energy in the part for $\theta_k \leq \theta \leq 180^\circ$. Since the shear load, P, plus the moment, Ph, will create the same bending moment as the clamping load on any specific cross section, it can be seen that the total internal energy in the segment is merely a function of the external load P.

If the deflections of several points in the bell cranks are desired, the following method is used to evaluate these deflections:

1. Select the points where the deflections are desired.

2. Divide the part into segments over which the cross sectional area can be assumed to be constant. Care should be taken to see that the points where the deflections are desired should fall on the boundary of one of these segments. The number of segments needed depends on the configuration of the part under construction.

3. Evaluate the total strain energy in each segment.

4. Evaluate the total rotation of each segment.

5. Choose the point, K, where the deflection is desired.

6. Calculate the total strain energy between the face on which K lies and the built in end from (5).

7. Calculate the total rotation of the face on which K is located from (4).

8. Equate $\left(\frac{P\delta_k}{2} + \frac{M c_k}{2}\right)$ to the strain energy from (6).
(M = Ph, see Fig. 3, p. 15)

9. Solve for δ_k.

The bending stress can now be obtained from consideration of equations (2) and (11).

$$f_b = \frac{c\,(r - r_1)}{(R + r)\,\theta}\,E$$

$$C = \frac{\text{Moment } \theta}{E\left[b_1 A + b_2 B + b_3 D\right]}$$

$$f_b = \frac{c\,(r - r_1)\,E}{(R + r)\,\theta} \tag{16}$$

$$= \frac{\text{Moment } \theta\,(r - r_1)\,E}{(R + r)\,\theta\,E\left[b_1 A + b_2 B + b_3 D\right]}$$

$$= \frac{\text{Moment } (r - r_1)}{(R + r)\left[b_1 A + b_2 B + b_3 D\right]}$$

Although the effect of the compressive or tensile loads were neglected in the deflection analysis, their effect on the stress can be evaluated where

$$\Delta f = \pm \frac{P_n}{A} \quad \begin{cases} P_n \text{ is the component of P normal} \\ \text{to the area under consideration} \end{cases} \tag{17}$$

The total stress at $r = r_o$ is then:

$$f = f_b + \Delta f = \frac{\text{Moment } (r_o - r_1)}{(R + r_o)\left[b_1 A + b_2 B + b_3 D\right]} \pm \frac{P_n}{A} \tag{18}$$

The $\pm$ is used to denote the fact that the load P could create a tensile or compressive force depending on the segment under consideration.

CHAPTER IV

EXPERIMENTAL TESTS

Stress-Strain Diagram.--The only properties of the material needed in the calculation of deflections is E, the modulus of elasticity, and the proportional limit. Two test bars were cast along with the bell cranks used in this analysis. The test bars were machined to the following specifications:

1. Test length = 2 inches
2. Test diameter = 0.5 inches

This test was run on a Tinius-Olsen tensile testing machine. The elongation was measured with the Tinius-Olsen Atcotran, an electronic strain gauge, which was part of the equipment of the machine. A plot of load versus strain was plotted on the Tinius Recorder. Using the cross sectional dimensions from above, the load was transformed to stress and a plot of stress versus strain was obtained (ref. Fig. 4, p. 6).

It can be seen from the graph of stress versus strain that the elastic range extends to 12,000 psi. The value for E can now be obtained, where $E = \frac{\Delta f}{\Delta \epsilon}$ (see p. 21).

Deflections.--The two bell cranks were cut as shown in Fig. 1, page 1. They were then mounted in the compression stand and subjected to compressive loads ranging from zero to 180 pounds. The compression machine used in this experiment read from zero to 200 pounds, in 0.2 pound increments, but the maximum load imposed on the bell cranks was restricted to 180

pounds since the machine had to be zeroed at 20 pounds.

Several small holes were drilled symmetrically in the upper and lower half of each cast part where the deflections were to be found. The Riehle Extensometer was used to measure the actual deflections. The Extensometer was incorporated into the system by extending it to its fully extended length; compression then could be determined by reading the scale backwards. This scale was graduated in 0.0002 inch increments. The Extensometer was mounted on the Extension Mount as shown in Fig. 5, p. 6.

The results of these tests are shown in Fig. 11, p. 26, and Fig. 15, p. 32. These results verify the assumption that deflections are linear functions of the external loading. It should also be noted that the curves do not pass through the origin in any case. This is explained by the fact that there was some initial play in the system used to measure the deflections. This play can be evaluated, for it is the distance between the origin and the intercept of the graph on the deflection axis. The true deflection curve can now be obtained by drawing another curve that is parallel to the original curve and passes through the origin. This correction is made in the plot of measured deflections versus theoretical deflections on pages 40 and 47.

Stresses.--SR-4, AD-7 strain gauges were mounted in each part to determine the stress at selected stations. Readings for strain were taken, where the clamping load varied from zero to 180 pounds, on an SR-4 strain gauge indicator. These readings are in ϵ directly and can be converted to stress by the equation: $f = \epsilon E$. The procedure used here is the standard one for determining stress with strain gauges and no detailed explanation will

be presented for this reason. This procedure is explained in Ref. 1. The results of this experiment are shown in Fig. 12, p. 28, and Fig. 16, p. 34. The selected stations are shown in Fig. 10, p. 23, and Fig. 14, p. 30. The dimensions and divisions of both parts are shown on pages 22 and 29.

The results of the experimental tests are shown on the following pages.

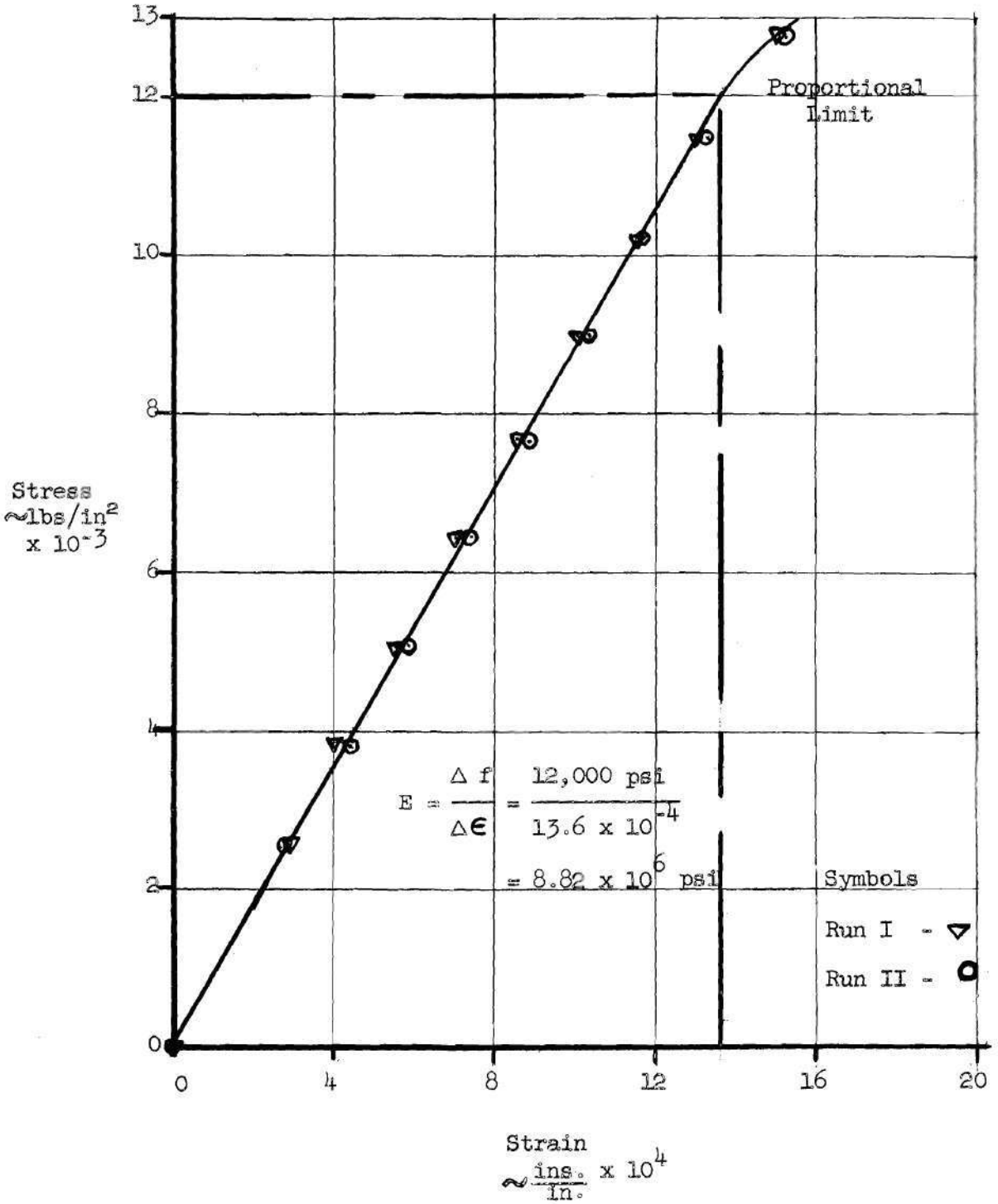

Fig. 8 Stress-Strain Diagram

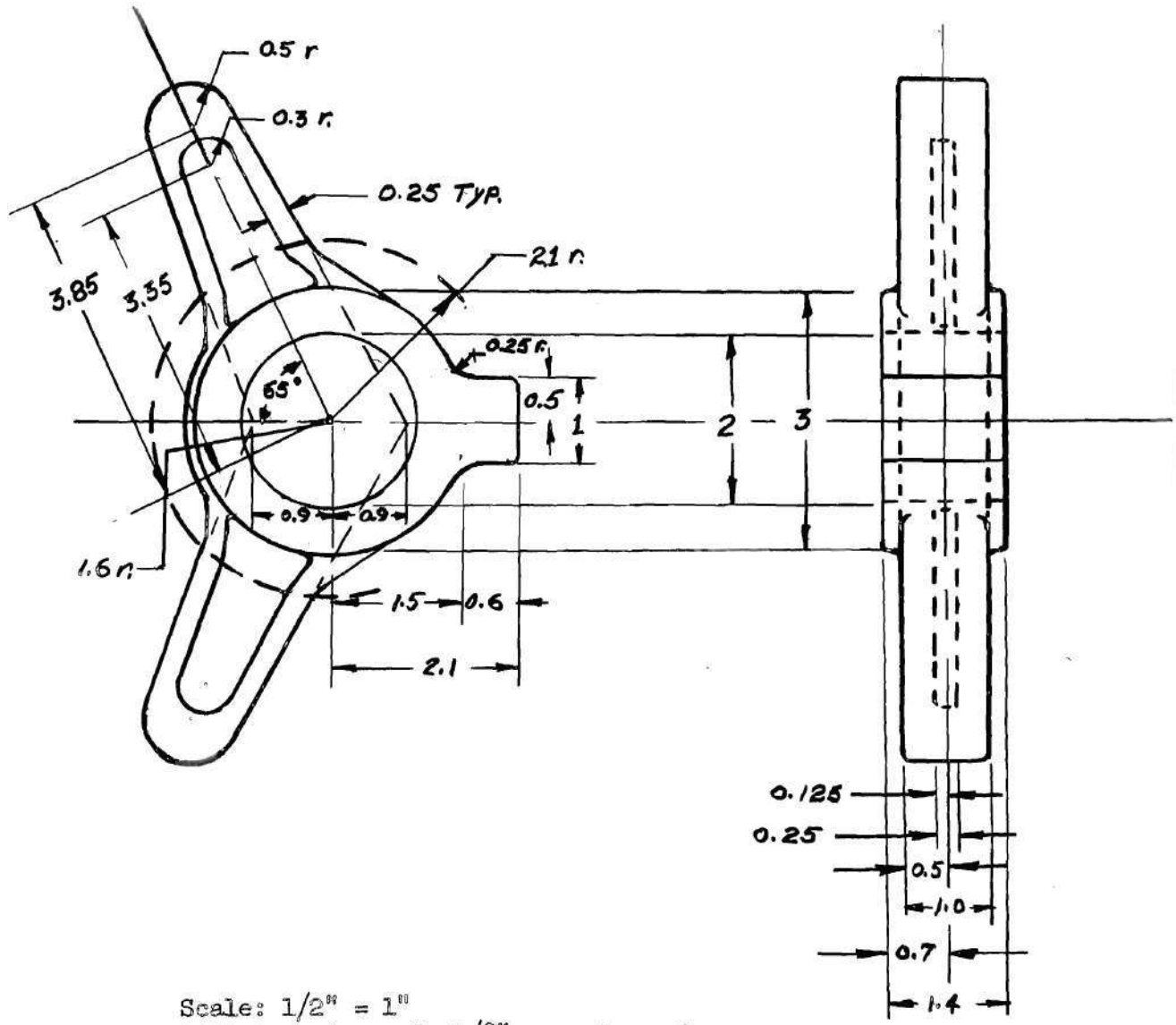

Scale: 1/2" = 1"
Fillets and rounds 1/8" except as shown

Fig. 9 Dimensions of Part I

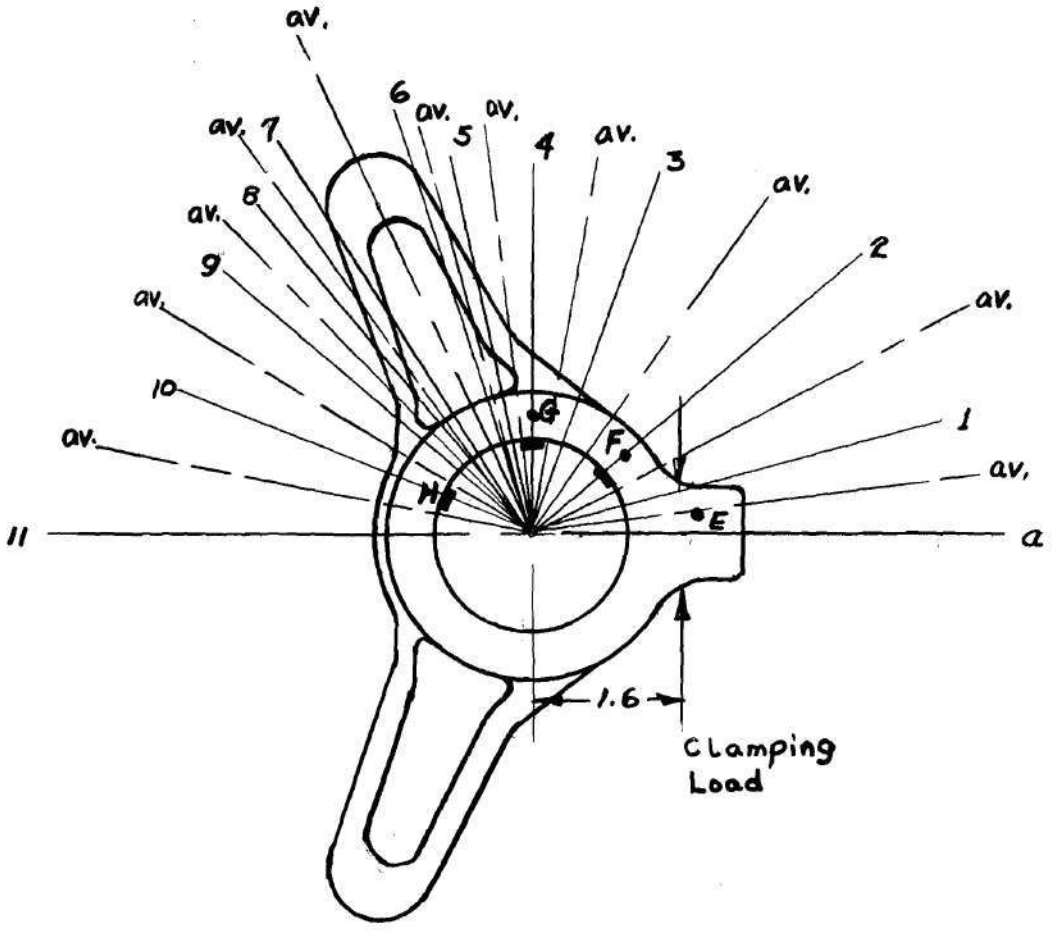

Note: Solid lines are the boundary lines of the sections over which the cross sectional properties are constant. The cross sectional properties of the average section is used.

Symbols: ▬ Strain Gauge

• Point for calculating deflection

Fig. 10 Division of Part I

Table 1. Experimental Data for Loads and Deflections - Part I

Point E

Load	δ - Run I	δ - Run II	δ - Run III	δ - Run IV
lbs.	ins. x 10^3	ins. x 10^3	ins. x 10^3	ins. x 10^3
0	0	0	0	0
20	0.9	0.6	0.6	0.5
40	2.6	2.2	2.4	2.2
60	4.1	4.0	4.0	3.8
80	5.7	5.6	5.6	5.6
100	7.4	7.0	7.0	7.2
120	8.9	8.8	8.6	8.8
140	10.4	10.4	10.0	10.2
160	12.1	11.8	11.6	12.0
180	13.5	13.8	13.1	13.4

Point G

Load	δ - Run I	δ - Run II	δ - Run III	δ - Run IV
lbs.	ins. x 10^3	ins. x 10^3	ins. x 10^3	ins. x 10^3
0	0	0	0	0
20	0.1	0.2	0.2	0.1
40	0.4	0.7	0.6	0.4
60	0.9	1.0	1.1	1.0
80	1.4	1.5	1.7	1.5
100	2.0	2.1	2.0	2.0
120	2.4	2.6	2.3	2.4
140	2.8	3.1	2.7	3.1
160	3.3	3.8	3.2	3.6
180	3.9	4.4	3.8	4.0

Table 1. Experimental Data for Loads and Deflections - Part I

(continued)

Point F

Load	δ - Run I	δ - Run II	δ - Run III	δ - Run IV
lbs.	ins. x 10^3	ins. x 10^3	ins. x 10^3	ins. x 10^3
0	0	0	0	0
20	1.0	0.9	0.6	0.7
40	2.6	2.1	1.8	2.4
60	3.9	3.6	3.0	3.4
80	4.9	4.9	4.2	4.6
100	6.1	6.0	5.4	5.7
120	7.3	7.1	6.6	7.1
140	7.9	8.2	7.8	8.1
160	9.2	9.4	9.0	9.2
180	10.3	10.6	10.3	10.5

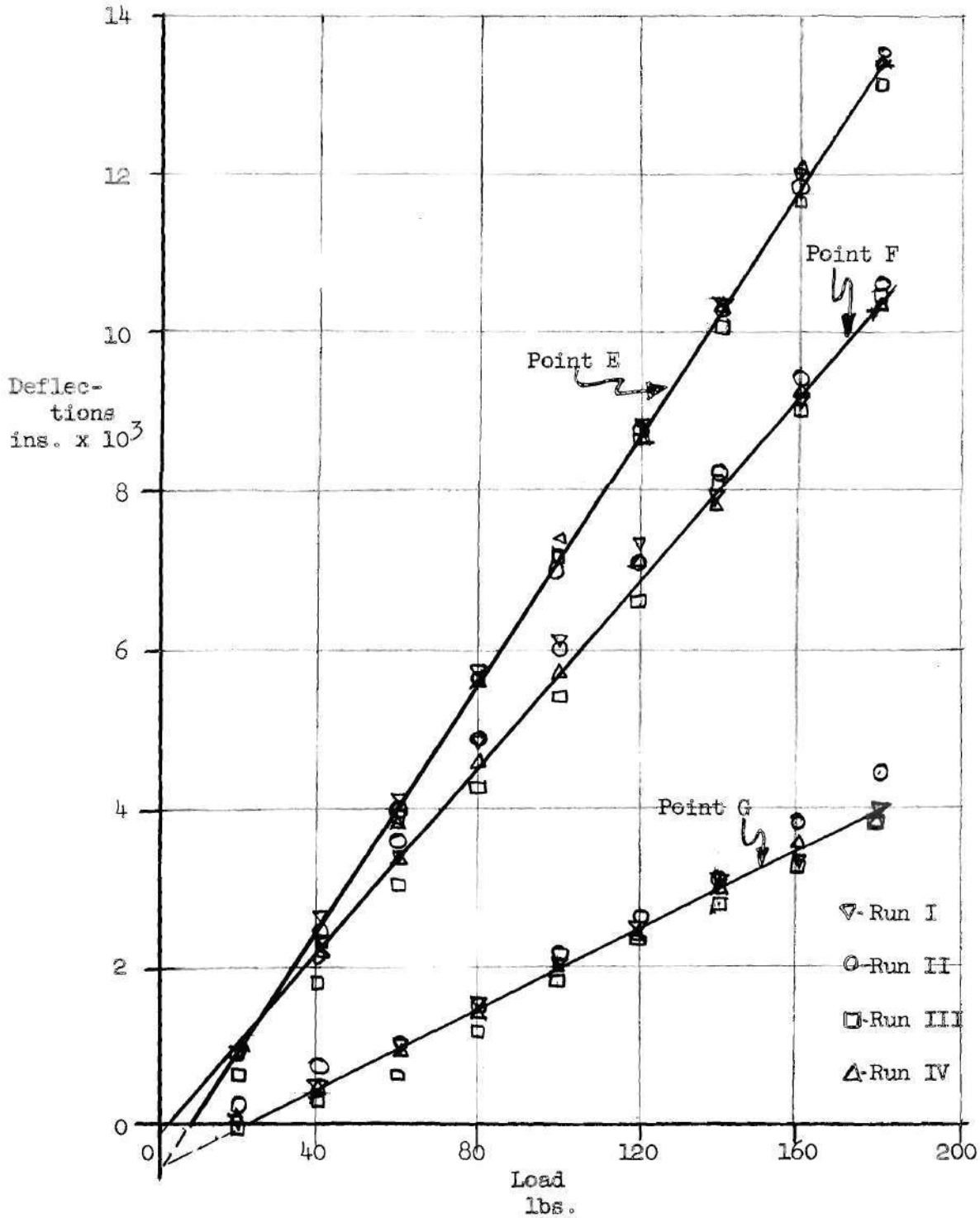

Fig. 11 Deflections of Part I

Table 2. Stresses - Part I

Points F, G, and H

Point	Loads	Run I		Run II		Run III		Run IV	
		ϵ	f	ϵ	f	ϵ	f	ϵ	f
	lbs.	$\frac{ins.}{in}(10^6)$	psi	$\frac{ins.}{in}(10^6)$	psi	$\frac{ins.}{in}(10^6)$	psi	$\frac{ins.}{in}(10^6)$	psi
F	0	0	0	0	0	0	0	0	0
	40	-35	-309	-40	-353	-37	-326	-37	-326
	80	-75	-662	-70	-618	-70	-618	-70	-618
	120	-105	-927	-105	-927	-102	-900	-102	-900
	160	-139	-1,230	-143	-1,260	-137	-1,210	-137	-1,210
	180	-155	-1,370	-160	-1,410	-152	-1,340	-152	-1,340
G	0	0	0	0	0	0	0	0	0
	40	-70	-617	-71	-626	-70	-617	-75	-661
	80	-145	-1,280	-140	-1,235	-140	-1,235	-155	-1,370
	120	-211	-1,860	-211	-1,860	-210	-1,850	-220	-1,940
	160	-282	-2,490	-285	-2,520	-280	-2,480	-290	-2,560
	180	-310	-2,740	-320	-2,820	-318	-2,800	-325	-2,870
H	0	0	0	0	0	0	0	0	0
	40	-190	-1,680	-185	-1,630	-197	-1,740	-185	-1,630
	80	-364	-3,210	-355	-3,140	-352	-3,110	-360	-3,180
	120	-550	-4,850	-530	-4,680	-522	-4,600	-535	-4,720
	160	-720	-6,350	-715	-6,310	-702	-6,200	-715	-6,310
	180	-815	-7,190	-805	-7,100	-802	-7,070	-802	-7,070

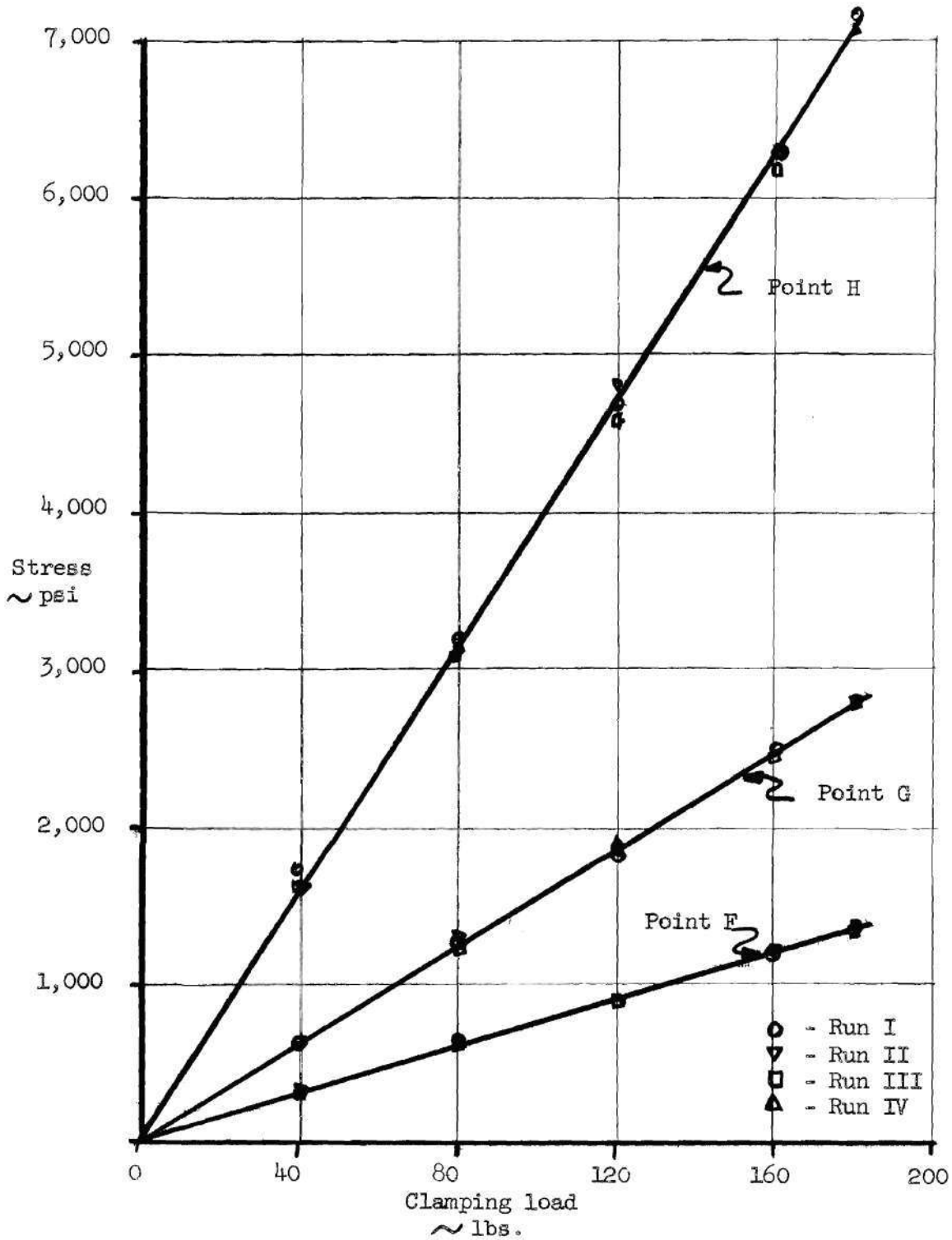

Fig. 12 Experimental Stresses - Part I

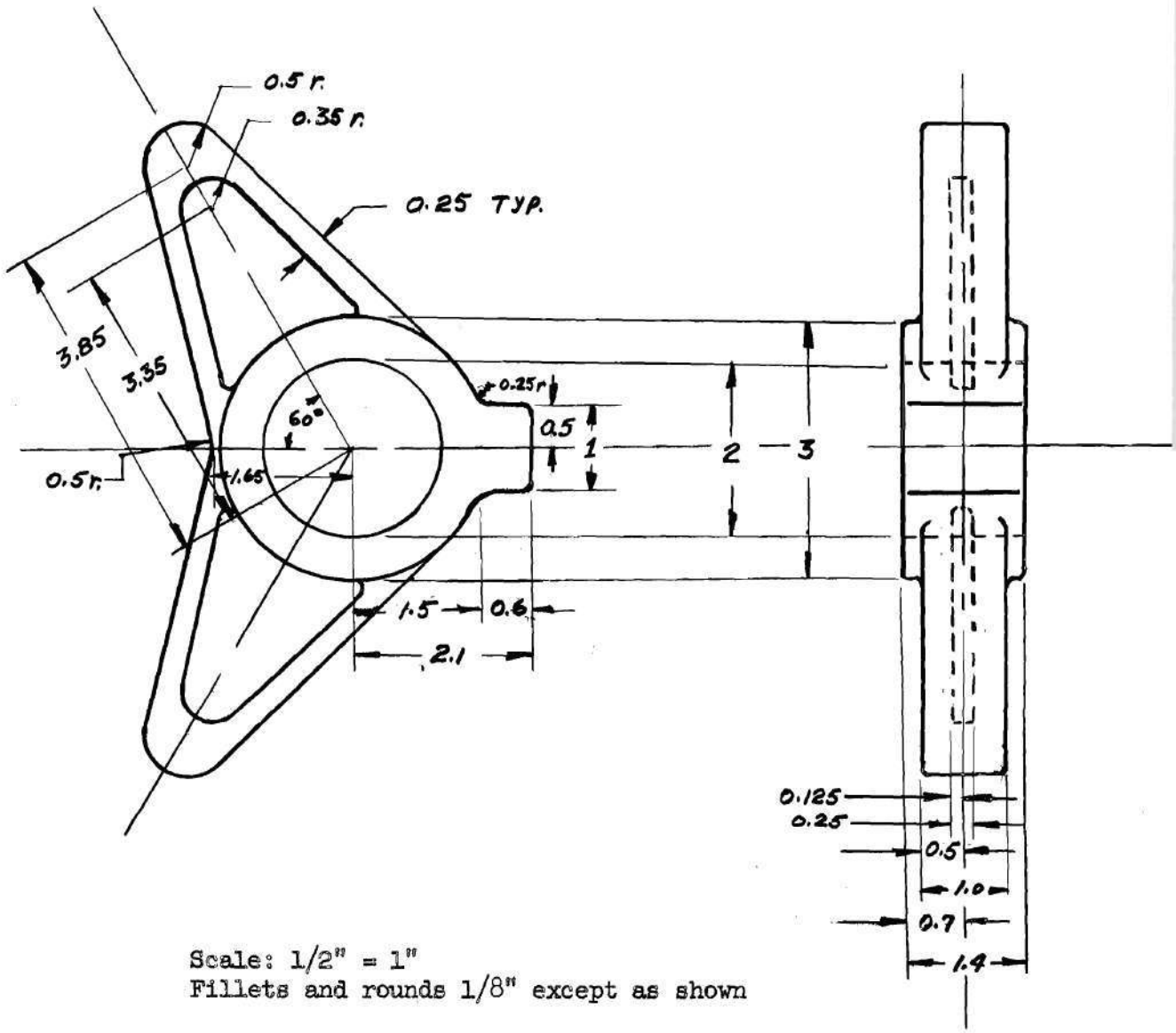

Scale: 1/2" = 1"
Fillets and rounds 1/8" except as shown

Fig. 13 Dimensions of Part II

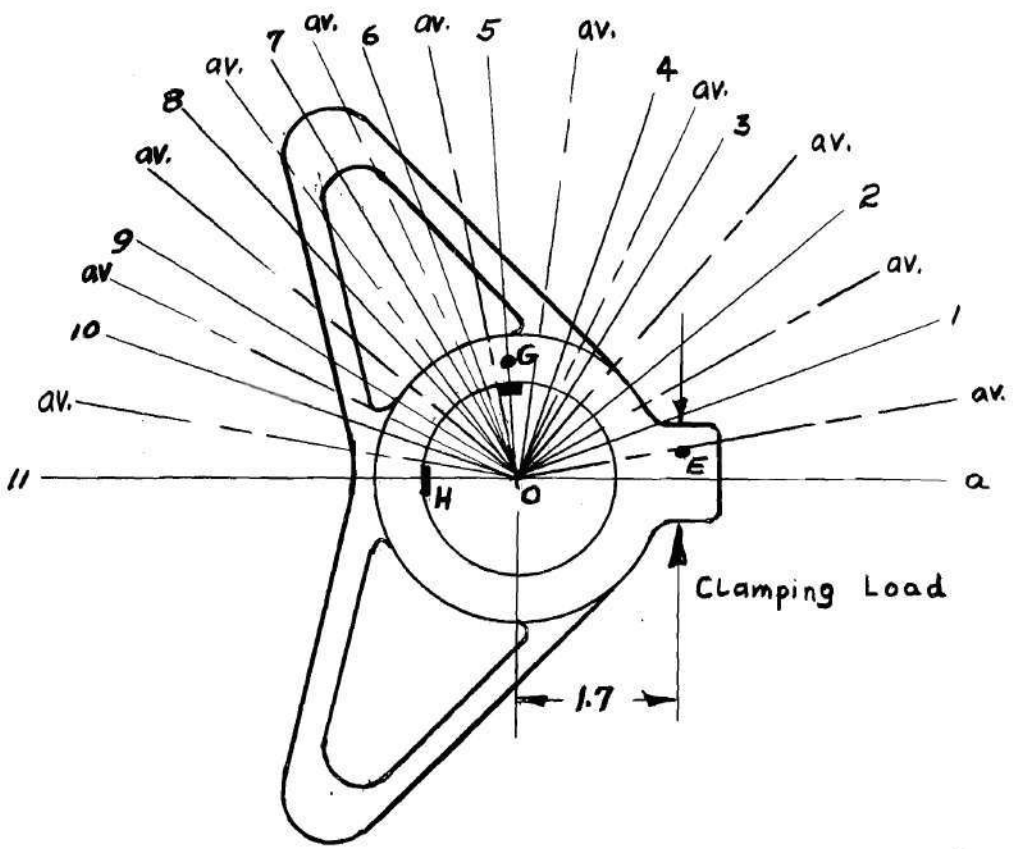

Note: Solid lines are the boundary lines of the sections over which the cross sectional properties are constant. The cross sectional properties of the average section are used.

Symbols: ▬ Strain Gauge

● Point for calculating deflection.

Fig. 14 Division of Part II

Table 3. Experimental Data for Loads and Deflections - Part II

Point E

Load	δ - Run I	δ - Run II	δ - Run III	δ - Run IV
lbs.	ins. x 10^3	ins. x 10^3	ins. x 10^3	ins. x 10^3
0	0	0	0	0
20	0.8	0.4	0.4	0.5
40	1.8	1.4	1.5	1.6
60	2.9	2.4	2.6	2.8
80	3.9	3.6	3.8	3.8
100	5.2	4.8	4.9	4.8
120	6.4	5.9	6.0	6.0
140	7.7	7.2	7.2	7.2
160	8.6	8.4	8.5	8.2
180	9.6	9.5	9.6	9.4

Point G

Load	δ - Run I	δ - Run II	δ - Run III	δ - Run IV
lbs.	ins. x 10^3	ins. x 10^3	ins. x 10^3	ins. x 10^3
0	0	0	0	0
20	0.2	0.1	0.1	0.1
40	0.4	0.3	0.4	0.5
60	0.8	0.7	0.7	0.9
80	1.2	1.1	1.0	1.1
100	1.5	1.4	1.4	1.4
120	1.9	1.9	1.9	1.7
140	2.3	2.2	2.2	2.0
160	2.6	2.5	2.6	2.4
180	3.0	3.0	3.0	2.8

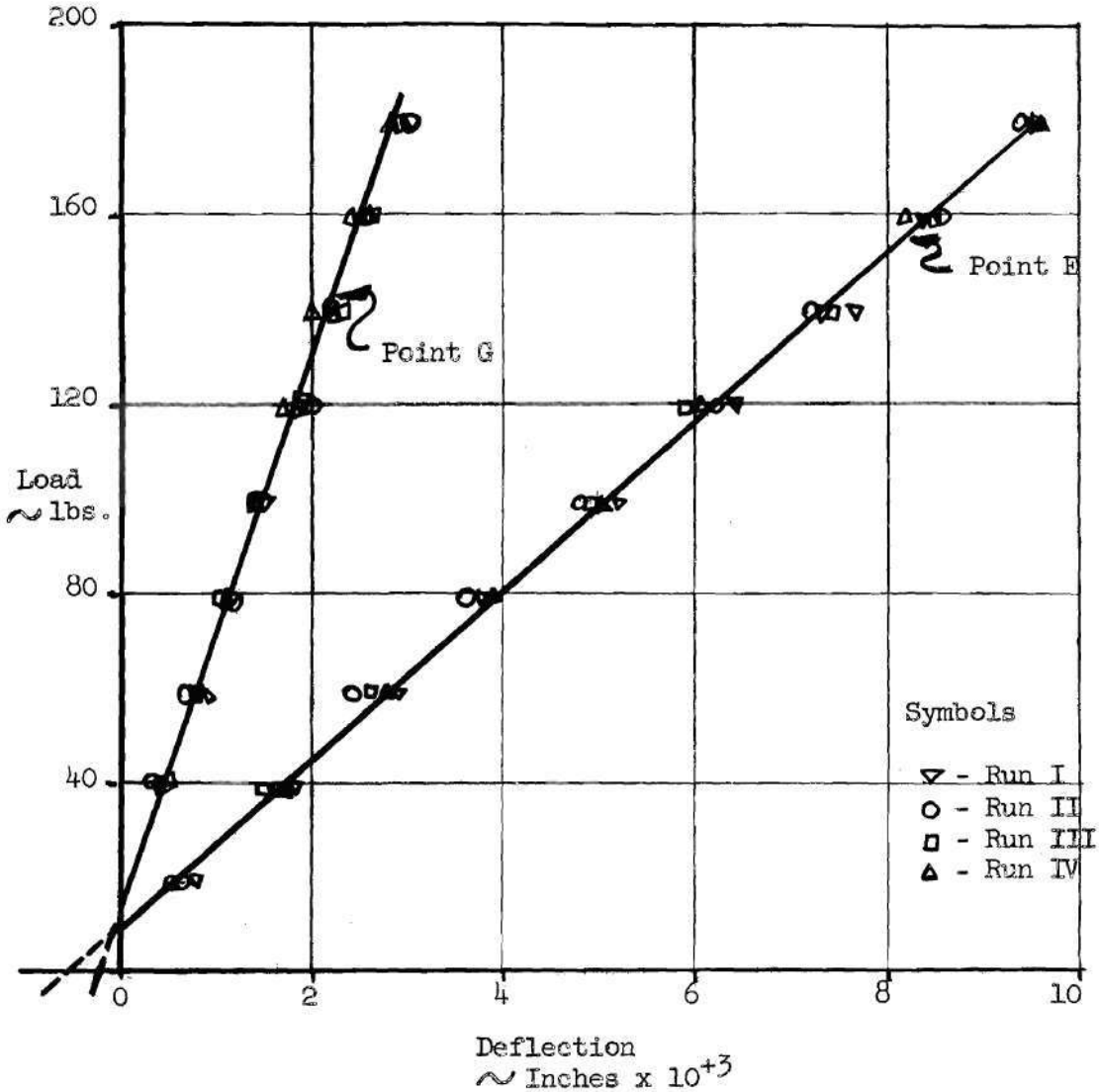

Fig. 15 Deflections of Part II

Table 4. Stresses - Part II

Points F, G, and H

Point	Loads	Run I		Run II		Run III		Run IV	
		ϵ	f	ϵ	f	ϵ	f	ϵ	f
	lbs.	$\frac{ins.}{in}(10^6)$	psi	$\frac{ins.}{in}(10^6)$	psi	$\frac{ins.}{in}(10^6)$	psi	$\frac{ins.}{in}(10^6)$	psi
G	0	0	0	0	0	0	0	0	0
	40	-45	-397	-42	-370	-40	-353	-42	-370
	80	-86	-760	-82	-725	-86	-760	-90	-795
	120	-130	-1,145	-122	-1,075	-118	-1,040	-127	-1,120
	160	-170	-1,500	-163	-1,440	-166	-1,460	-172	-1,520
	180	-193	-1,700	-190	-1,680	-186	-1,164	-193	-1,700
H	0	0	0	0	0	0	0	0	0
	40	-160	-1,410	-151	-1,330	-145	-1,280	-153	-1,350
	80	-300	-2,650	-300	-2,650	-309	-2,730	-300	-2,650
	120	-440	-3,880	-445	-3,920	-440	-3,880	-443	-3,910
	160	-598	-5,280	-590	-5,200	-593	-5,230	-595	-5,250
	180	-690	-6,100	-676	-5,960	-683	-6,020	-684	-6,030

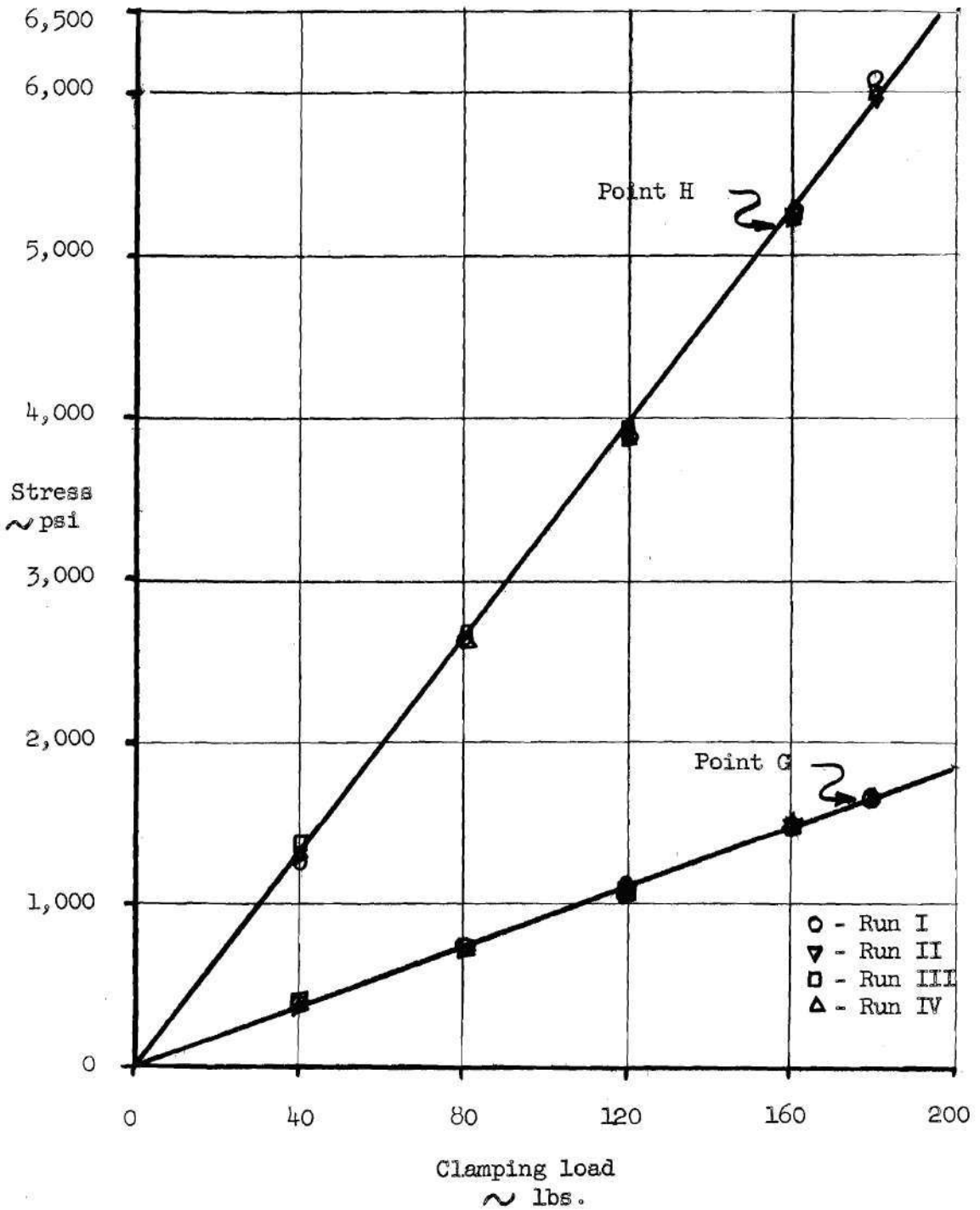

Fig. 16 Experimental Stresses - Part II

CHAPTER V

ANALYTICAL SOLUTIONS OF DEFLECTIONS AND STRESSES

The strain energy and rotation of each segment, over which the cross sectional properties are assumed to be constant, can be evaluated in tabular form as outlined on page 16. The tables for both parts are included in the following pages and a column explanation is given on page 42.

The deflections are found by equating the internal strain energy to the external energy obtained from the clamping load.

The strain gauges have been mounted so that they are divided in half by the boundary between two segments of the bell crank. The computation of the average stress can best be explained by an example. Point G, at $\theta = 94^{o}$, of Part II is used (Ref. p. 46).

The strain gauge was mounted so that it extended into segments 4-0-5 and 5-0-6. The stress can then be seen to be a function of the properties of segments 4-0-5 and 5-0-6.

The stress can be computed using eq. 18, p. 17, assuming that it is the average of the stresses obtained using the properties of segments 4-0-5 and 5-0-6 individually. The moment is assumed to act about the location of r_1 for each segment on the meridional line, $\theta = 94^{o}$.

$\Delta f_{b_{4-0-5}}$ is the stress obtained using the properties of section 4-0-5 in eq. 18. A similar definition is used for $\Delta f_{b_{5-0-6}}$.

$$f_{b_{a.v}} = \frac{\Delta f_{b_{4-0-5}} + \Delta f_{b_{5-0-6}}}{2} + \frac{P_n}{\frac{A_{4-0-5} + A_{5-0-6}}{2}}$$

$P_n = P \cos 94^o$

A = Area of the indicated cross sections

In this particular segment:

$\Delta f_{b_{4-0-5}} = -2220$ psi

$\Delta f_{b_{5-0-6}} = -1090$ psi

P_n is neglected

$$f_{av} = \frac{-2220 - 1090}{2} = -1655 \text{ psi}$$

Table 5. Strain Energy - Part I

1	2	3	4	5	6	7	8	9	10
Segment	θ_1	θ_2	b_1	b_2	b_3	t_1	t_2	t_3	r_1
	degrees	degrees	ins.	ins.	ins.	ins.	ins.	ins.	ins.
a-0-1	0	15	1.4	0	0	1.18	0	0	0.514
1-0-2	15	40	1.4	0	0	0.60	0	0	0.276
2-0-3	40	70	1.4	0	0	0.50	0	0	0.235
3-0-4	70	90	1.4	1.00	0	0.50	0.70	0	0.300
4-0-5	90	102	1.4	1.00	0	0.50	1.15	0	0.450
5-0-6	102	108	1.4	0.25	1.0	0.50	1.00	1.60	0.580
6-0-7	108	122	1.4	0.25	1.0	0.50	2.60	3.35	1.020
7-0-8	122	129	1.4	0.25	1.0	0.50	1.20	2.00	0.720
8-0-9	129	139	1.4	1.00	0	0.50	1.10	0	0.435
9-0-10	139	157	1.4	1.00	0	0.50	0.70	0	0.300
10-0-11	157	180	1.4	1.00	0	0.5	0.60	0	0.265

11	12	13	14	15	16	17
Segment	A	B	D	$\frac{dc}{M\,d\theta}\,E$	$\frac{E}{P^2}\int_{\theta_1}^{\theta_2}\frac{M\,dc}{2}$	$\frac{E}{P}\int_{\theta_1}^{\theta_2} dc$
				$\frac{1}{ins^3}$	$\frac{1}{ins.}$	$\frac{1}{ins^2}$
a-0-1	0.2608	-	-	2.74	0.01	0.08
1-0-2	0.0140	-	-	51.10	2.58	10.60
2-0-3	0.0084	-	-	85.00	18.70	39.80
3-0-4	0.0110	0.010	-	39.40	13.20	19.00
4-0-5	0.0270	0.058	-	10.45	2.27	3.95
5-0-6	0.0550	0.012	0.135	4.65	1.23	0.93
6-0-7	0.2650	0.427	0.737	0.82	0.78	0.50
7-0-8	0.1050	0.025	0.245	2.55	1.11	0.81
8-0-9	0.0250	0.050	-	11.80	5.75	5.33
9-0-10	0.0110	0.010	-	39.40	45.00	33.40
10-0-11	0.0090	0.003	-	64.00	102.00	72.70

(see p. 42 for a column explanation)

Calculated Deflections for Part I

Point E

$$\frac{P\,\delta_E}{2} = \sum \text{Internal strain energy for } 0^\circ \leq \theta \leq 180^\circ$$

$$= 192.63\,\frac{P^2}{E}$$

$$\delta_E = 385.26\,\frac{P}{E} = 43.7\,P \times 10^{-6}$$

This constitutes the deflection for the upper half only.

$$\delta_{E\ \text{Total}} = 2(43.7)\,P \times 10^{-6} = 87.4\,P \times 10^{-6}$$

For P = 180 lbs.

$$\delta_{E\ \text{Total}} = 87.4(180) \times 10^{-6} = .0157 \text{ ins.}$$

Point F

$$\frac{P\,\delta_F}{2} + \frac{M\,c_F}{2} = \sum \text{Internal strain energy for } 40^\circ \leq \theta \leq 180^\circ$$

$$M = P(1.6 - 1.276 \cos 40^\circ) = P(1.6 - .975) = .675\,P$$

$$\frac{P\,\delta_F}{2} + \frac{0.675\,P\,(176.419\,P)}{2\,E} = 190.043\,\frac{P^2}{E}$$

$$\delta_F = (380.086 - 119.0)\,\frac{P}{E} = 29.6\,P \times 10^{-6}$$

$$\delta_{F\ \text{Total}} = 2\,\delta_{F\ \text{upper half}}$$

$$= 2(29.6\,P \times 10^{-6}) = 59.2\,P \times 10^{-6}$$

For P = 180 lbs.

$$\delta_{F\ \text{Total}} = 59.2(180) \times 10^{-6} = .01065 \text{ ins.}$$

Point G

$$\frac{P\delta_G}{2} + \frac{M c_G}{2} = \leq \text{Internal energy for } 90^\circ \leq \theta \leq 180^\circ$$

$$M = P(1.6 - 1.3 \cos 90^\circ) = 1.6\,P$$

$$\frac{P\delta_G}{2} + 1.6\,P\,\frac{(117.619\,P)}{2\,E} = 158.15\,\frac{P^2}{E}$$

$$\delta_G = (316.3 - 188)\,\frac{P}{E} = 14.55\,P \times 10^{-6}$$

$$\delta_{G\ \text{Total}} = 2\,\delta_{G\ \text{upper half}}$$

$$= 2(14.55\,P \times 10^{-6}) = 29.1\,P \times 10^{-6}$$

For P = 180 lbs.

$$\delta_{G\ \text{Total}} = 29.1\,(180) \times 10^{-6} = .00524 \text{ ins.}$$

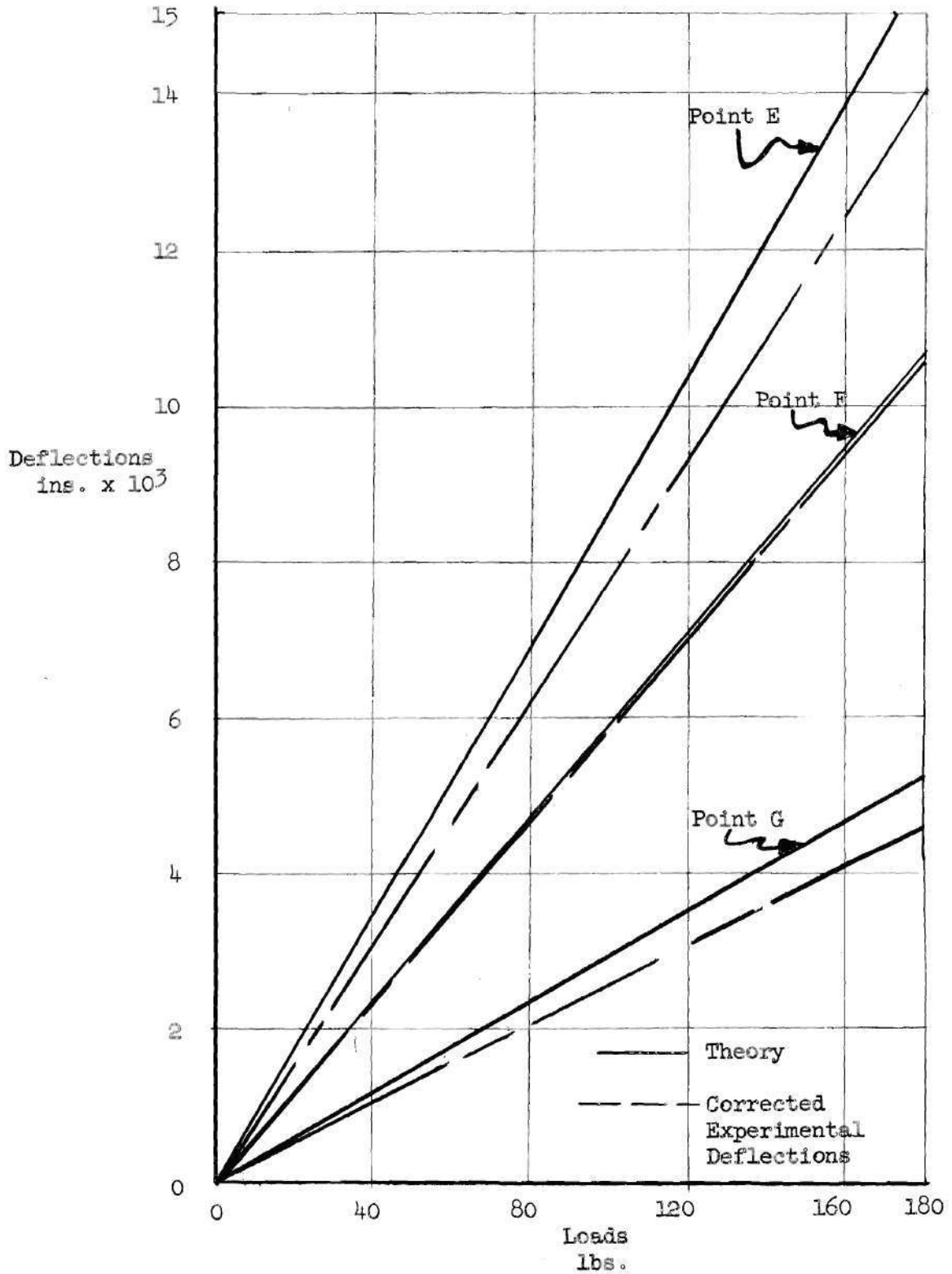

Fig. 17 Comparison of Corrected Deflections With Calculated Deflections for Part I

Table 6. Strain Energy - Part II

1	2	3	4	5	6	7	8	9	10
Segment	θ_1	θ_2	b_1	b_2	b_3	t_1	t_2	t_3	r_1
	degrees	degrees	ins.	ins.	ins.	ins.	ins.	ins.	ins.
a-0-1	0	21	1.4	0	0.	1.15	0	0	0.502
1-0-2	21	40	1.4	0	0	0.50	0	0	0.235
2-0-3	40	59	1.4	0	0	0.50	0	0	0.235
3-0-4	59	71	1.4	1.00	0	0.50	0.6	0	0.265
4-0-5	71	94	1.4	1.00	0	0.50	0.9	0	0.363
5-0-6	94	110	1.4	0.25	1.0	0.50	1.2	1.8	0.835
6-0-7	110	120	1.4	0.25	1.0	0.50	2.5	3.2	0.970
7-0-8	120	132	1.4	0.25	1.0	0.50	2.5	3.2	0.970
8-0-9	132	148	1.4	0.25	1.0	0.50	1.2	1.7	0.570
9-0-10	148	160	1.4	1.00	0	0.50	1.0	0	0.400
10-0-11	160	180	1.4	1.00	0	0.50	0.7	0	0.300

11	12	13	14	15	16	17
Segment	A	B	D	$\frac{dc\ E}{M\ d\theta}$	$\frac{E}{P^2}\int_{\theta_1}^{\theta_2}\frac{M\ dc}{2}$	$\frac{E}{P}\int_{\theta_1}^{\theta_2} dc$
				$\frac{1}{ins^3}$	$\frac{1}{ins.}$	$\frac{1}{ins^2}$
a-0-1	0.0830	-	-	8.60	0.24	0.696
1-0-2	0.0084	-	-	85.00	5.57	17.800
2-0-3	0.0084	-	-	85.00	11.53	24.600
3-0-4	0.0090	0.003	-	64.00	9.20	15.800
4-0-5	0.0220	0.022	-	19.50	11.45	12.000
5-0-6	0.1550	0.035	0.104	3.03	1.77	1.720
6-0-7	0.2300	0.405	0.937	0.74	1.04	0.770
7-0-8	0.2300	0.405	0.937	0.74	1.04	0.770
8-0-9	0.0550	0.041	0.160	4.05	4.62	3.260
9-0-10	0.0200	0.037	-	15.4	14.05	9.600
10-0-11	0.0110	0.0105	-	38.6	59.50	40.000

(see p. 42 for a column explanation)

Column Explanation for Tables

1. Segment - Division of the parts over which the cross sectional properties are assumed to be constant.

2. θ_1 - Lower angular limit of the segment.

3. θ_2 - Upper angular limit of the segment.

4. b_1
5. b_2
6. b_3
7. t_1
8. t_2
9. t_3

- Dimensions of the cross section (see page 8).

10. r_1 - Location of the neutral axis measured from the concave side (see page 8).

11. Segment - Same as 1.

12. $$A = \left[\frac{(R + t_1)^2}{2} - \frac{R^2}{2} - 2 R t_1 + (R + r_1)^2 \ln \frac{R + t_1}{R} - 2 r_1 t_1 \right]$$

13. $$B = \left[\frac{(R + t_2)^2}{2} - \frac{(R + t_1)^2}{2} + 2 (R + r_1)(t_1 - t_2) + (R + r_1)^2 \ln \frac{R + t_2}{R + t_1} \right]$$

14. $$D = \left[\frac{(R + t_3)^2}{2} - \frac{(R + t_2)}{2} + 2 (R + r_1)(t_2 - t_3) + (R + r_1)^2 \ln \frac{R + t_3}{R + t_2} \right]$$

(Note: R = 1 inch for both parts.)

15. $\frac{dc\ E}{M d\theta}$ - From eq. (11) $dc = \frac{\text{Moment } d\theta}{E\left[b_1 A + b_2 B + b_3 D\right]}$

$$\therefore \quad \frac{dc\ E}{M d\theta} = \frac{1}{\left[b_1 A + b_2 B + b_3 D\right]}$$

16. $\frac{E}{P^2}\int_{\theta_1}^{\theta_2} \frac{M\ dc}{2}$ - The strain energy in a segment is given by eq. (13):

$$\text{Strain energy} = \int_{\theta_1}^{\theta_2} \frac{M\ dc}{2}$$

$$= \int_{\theta_1}^{\theta_2} \frac{(\text{Moment})^2\ d\theta}{2E\left[b_1 A + b_2 B + b_2 D\right]}$$

When this integral is evaluated, the result will be in the form

$$\text{Strain energy} = \frac{P^2}{E}(\text{Constant})$$

In order to eliminate the need of carrying the $\frac{P^2}{E}$ term throughout the column, it has been divided out. Column 16 gives the value of the constant term for each segment.

17. $\frac{E}{P}\int_{\theta_1}^{\theta_2} d\ c$ The total rotation of each segment can be found from the following integral

$$c = \int_{\theta_1}^{\theta_2} dc = \int_{\theta_1}^{\theta_2} \frac{(\text{Moment})\ d\theta}{E\left[b_1 A + b_2 B + b_3 D\right]}$$

When this integral is evaluated, the rotation will be in the form:

$$\text{Rotation} = \frac{P}{E} \text{ (constant)}$$

As in column 16, the term $\frac{P}{E}$ has been divided out and the constant term for each segment is given in column 17.

The table can now be used to find the rotation or displacement of any point in the part under consideration. As an example, consider point F of Part I (see page 38).

The clamping load is applied at a point 0.675 inches from F, therefore a freebody of section 0-2 would have an external load equal to P applied and also a moment equal to 0.675 P. These two loads can be thought of as external loads at point F on section 0-2. The amount of external work applied to the part would be $\frac{P\delta_F}{2} + \frac{M c_F}{2}$, where δ_F represents the vertical displacement of point F and c_F represents the rotation of section 0-2. θ for section 0-2 is 40°.

The amount of internal strain energy can be evaluated from column 16 by taking the sum of the strain energies for the segments from $40^\circ \leq \theta \leq 180^\circ$. The rotation of face 0-2 can be evaluated from column 17 by adding the rotations of all the segments from $40^\circ \leq \theta \leq 180^\circ$. δ_F now is the only unknown and it can be determined (for the numerical solution see page 38).

Calculated Deflections for Part II

Point E

$$\frac{P\delta_E}{2} = \sum \text{Strain energy for } 0^\circ \leq \theta \leq 180^\circ$$

$$= 118.962 \frac{P^2}{E}$$

$$\delta_E = 237.924 \frac{P}{E} = 26.9\ P \times 10^{-6}$$

This represents the deflection for the upper half only.

$$\delta_{E\ \text{Total}} = 2(26.9\ P) \times 10^{-6} = 53.8\ P \times 10^{-6}$$

For P = 180 lbs.

$$\delta_{E\ \text{Total}} = 53.8(180) \times 10^{-6} = .0097 \text{ ins.}$$

Point F

$$\frac{P\delta_F}{2} + \frac{M c_F}{2} = \sum \text{Internal strain energy for } 40^\circ \leq \theta \leq 180^\circ$$

$$M = P(1.7 - 1.235 \cos 40^\circ) = P(1.7 - .945)$$

$$= 0.755\ P$$

$$\frac{P\delta_F}{2} + \frac{0.755\ P}{2}\left(\frac{108.65\ P}{E}\right) = 113.155 \frac{P^2}{E}$$

$$\delta_F = (226.31 - 82) \frac{P}{E} = 16.4\ P \times 10^{-6}$$

$$\delta_{F\ \text{Total}} = 2\ \delta_{F\ \text{upper half}} = 2\ (16.4\ P \times 10^{-6})$$

For P = 180 lbs.

$$\delta_{F\ \text{Total}} = 32.8(180) \times 10^{-6} = .0059 \text{ ins.}$$

Point G

$$\frac{P\delta_G}{2} + \frac{M\theta_G}{2} = \leq \text{Internal energy for } 94^\circ \leq \theta \leq 180^\circ$$

$$\text{Moment} = P(1.7 - 1.363 \cos 94^\circ) = P(1.7 + .095)$$

$$= 1.795\ P$$

$$\frac{P\delta_G}{2} + \frac{1.795\ P\ (55.35\ P)}{2\ E} = 80.975\ \frac{P^2}{E}$$

$$\delta_G = (161.95 - 99)\ \frac{P}{E} = 7.13\ P \times 10^{-6}$$

$$\delta_{G\ \text{Total}} = 2\ \delta_{G\ \text{upper half}} = 2(7.13\ P) \times 10^{-6}$$

$$= 14.26\ P \times 10^{-6}$$

For P = 180 lbs.

$$\delta_{G\ \text{Total}} = 14.26(180) \times 10^{-6} = .00256 \text{ ins.}$$

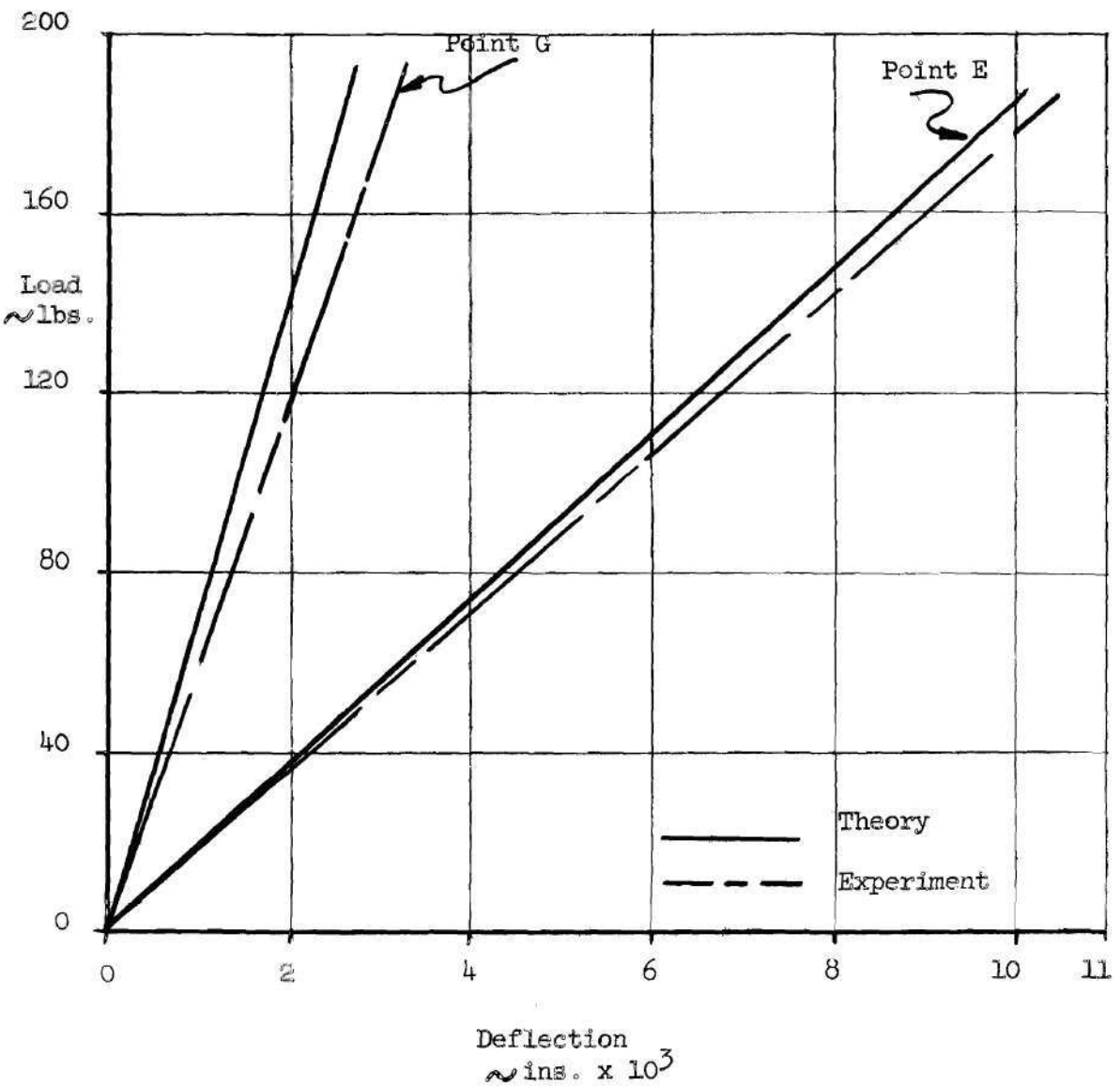

Fig. 18 Comparison of Corrected Deflections With Calculated Deflections for Part II

Stresses in Part I

Point F, $\theta = 40^{o}$

$$\Delta f_{b(1\text{-}0\text{-}2)} = \frac{(1.6 - 1.276 \cos 40^{o})(180)(-.276)}{1.4(.014)}$$

$$= -1,585 \text{ psi}$$

$$\Delta f_{b(2\text{-}0\text{-}3)} = \frac{(1.6 - 1.235 \cos 40^{o})(180)(-.235)}{1.4(.0084)}$$

$$= -2,360 \text{ psi}$$

$$f_{b_{av}} = \frac{\Delta f_{b(1\text{-}0\text{-}2)} + \Delta f_{b(2\text{-}0\text{-}3)}}{2}$$

$$= \frac{-1,585 - 2,360}{2} = -1,972$$

$$P_n = 180 \cos 40^{o} = 138 \text{ lbs.}$$

$$A_{av} = \frac{1.4(.6) + 1.4(.5)}{2} = .77 \text{ in}^2$$

$$\frac{P_n}{A_{av}} = \frac{138}{.77} = 179 \text{ psi}$$

$$f = f_{b_{av}} + \frac{P_n}{A_{av}} = -1,972 + 179 = -1,793 \text{ psi}$$

Point G, $\theta = 90^{o}$

$$\Delta f_{b(3\text{-}0\text{-}4)} = \frac{(1.6 - 1.3 \cos 90^{o})(180)(-.3)}{1.4(.011) + 1(.01)}$$

$$= -3400 \text{ psi}$$

$$\Delta f_{b(4\text{-}0\text{-}5)} = \frac{(1.6 - 1.45 \cos 90^{o})(180)(-.45)}{1.4(.027) + 1(.058)}$$

$$= -1350 \text{ psi}$$

$$f_{b_{av}} = \frac{\Delta f_{b(3\text{-}0\text{-}4)} + \Delta f_{b(4\text{-}0\text{-}5)}}{2}$$

$$= \frac{-3400 - 1350}{2} = -2375 \text{ psi}$$

$$P_n = 180 \cos 90^\circ = 0$$

Point H, $\theta = 157^\circ$

$$\Delta f_{b(9\text{-}0\text{-}10)} = \frac{(1.6 - 1.3 \cos 157^\circ)(180)(-.3)}{1.4(.011) + 1(.01)}$$

$$= -5940 \text{ psi}$$

$$\Delta f_{b(10\text{-}0\text{-}11)} = \frac{(1.6 - 1.265 \cos 157^\circ)(180)(-.265)}{1.4(.009) + 1(.003)}$$

$$= -8450$$

$$f_{b_{av}} = \frac{\Delta f_{b(9\text{-}0\text{-}10)} + \Delta f_{b(10\text{-}0\text{-}11)}}{2}$$

$$= \frac{-5,940 - 8,450}{2} = -7,195 \text{ psi}$$

$$P_n = 180 \cos 157^\circ = -166 \text{ lbs.}$$

$$A_{av} = \frac{\left[1.4(.5) + 1(.2)\right] + \left[1.4(.5) + 1.(.1)\right]}{2}$$

$$= 0.85 \text{ in}^2$$

$$\frac{P_n}{A_{av}} = \frac{-166}{0.85} = -195 \text{ psi}$$

$$f = f_{b_{av}} + \frac{P_n}{A_{av}} = -7,195 - 195$$

$$= -7,390 \text{ psi}$$

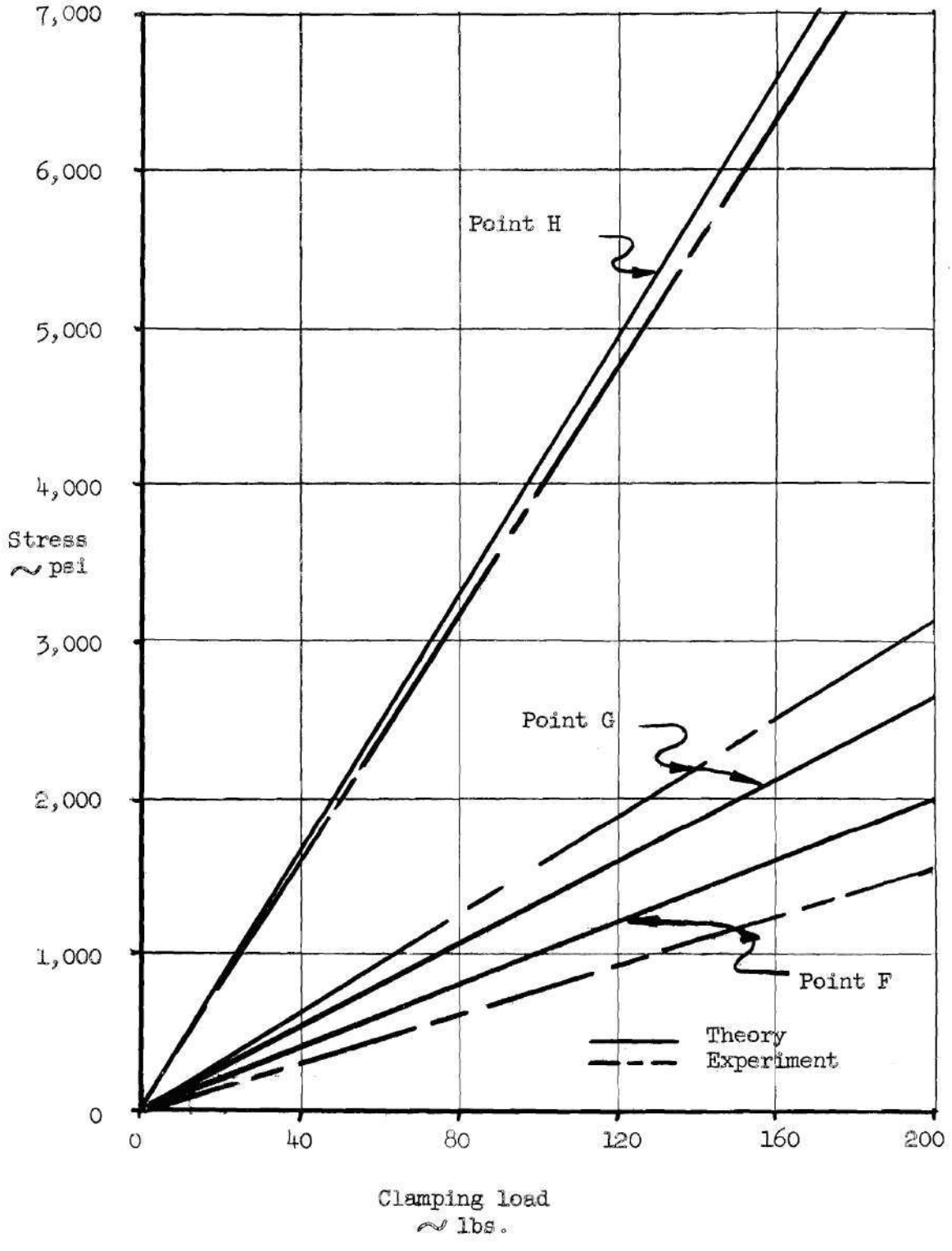

Fig. 19 Comparison of Theoretical and Experimental Stress - Part I

Stresses in Part II

Point G, $\theta = 94^{\circ}$

$$\Delta f_{b(4\text{-}0\text{-}5)} = \frac{(1.7 - 1.363 \cos 94^{\circ})(180)(-.363)}{1.4(.022) + 1(.022)}$$

$$= -2{,}220 \text{ psi}$$

$$\Delta f_{b(5\text{-}0\text{-}6)} = \frac{(1.7 - 1.835 \cos 94^{\circ})(180)(-.835)}{1.4(.155) + 1(.035)}$$

$$= -1{,}090$$

$$f_{b_{av}} = \frac{\Delta f_{b(4\text{-}0\text{-}5)} + \Delta f_{b(5\text{-}0\text{-}6)}}{2}$$

$$= \frac{-2{,}220 - 1{,}090}{2} = -1{,}655 \text{ psi}$$

$$P_n = 180 \cos 94^{\circ} = 12.6 \text{ lbs.}$$

P_n can be neglected here.

Point H, $\theta = 180^{\circ}$

$$f_b = \frac{(1.7 - 1.3 \cos 180^{\circ})(180)(-.3)}{1.4(.011) + 1(.0105)}$$

$$= -6{,}250 \text{ psi}$$

$$P_n = -180 \text{ lbs.}$$

$$\frac{P_n}{A} = -\frac{180}{0.9} = -200 \text{ psi}$$

$$f = f_b + \frac{P_n}{A} = -6{,}250 - 200$$

$$= -6{,}450 \text{ psi}$$

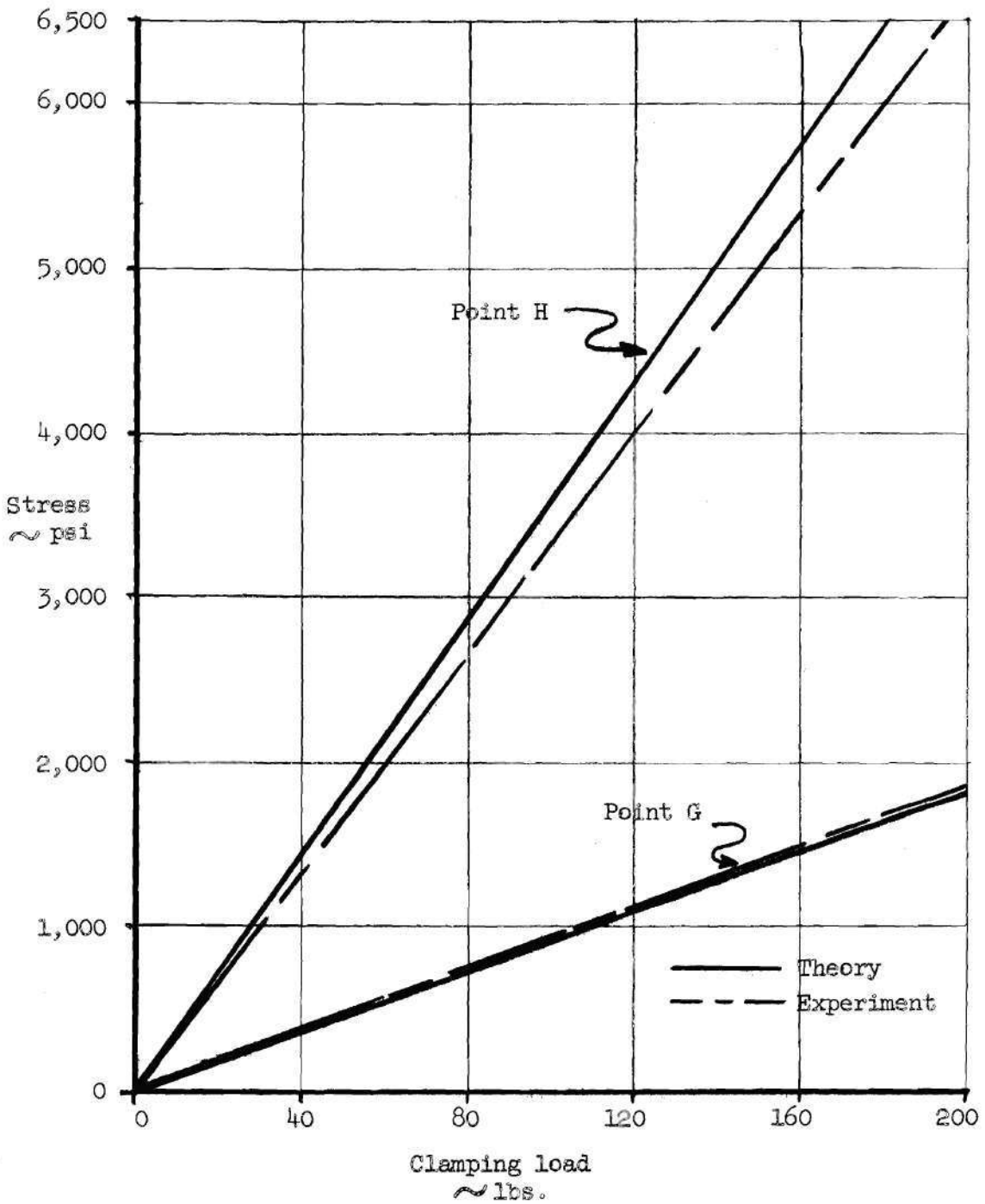

Fig. 20 Comparison of Theoretical and Experimental Stresses - Part II

CHAPTER VI

DISCUSSION OF RESULTS

Comparison of Theoretical and Experimental Deflections

The experimental results corroborate the assumption that the deflections are a linear function of the clamping load in the elastic range. A graphical comparison of the theoretical and experimental deflections is presented in Fig. 17, page 40 and Fig. 18, page 47. The maximum clamping load applied to both parts was 180 pounds, and the results are tabulated below.

Deflections--(inches)

Part I

Point	Theory	Experiment
E	0.0157	0.014
F	0.0106	0.0105
G	0.0046	0.0052

Part II

Point	Theory	Experiment
E	0.0097	0.0101
G	0.0026	0.0031

The average variation between the theoretical and measured deflections is slightly under nine per cent for the two parts. From this it can be seen that there is good correlation between the analytical solution and experiment.

Comparison of Theoretical and Experimental Stresses

The plots of theoretical versus experimental stresses are presented in Figs. 19 and 20 on pages 50 and 52 respectively.

The maximum stresses obtained at each point, under the 180 pound clamping load, are presented here.

Stresses (pounds per square inch)

Part I

Point	Theory	Experiment
F	1,800	1,400
G	2,400	2,800
H	7,400	7,100

Part II

Point	Theory	Experiment
G	1,640	1,650
H	6,450	6,000

The average variation between the theoretical and measured stresses is 9.6 per cent, which again shows good correlation between the theory and experiment for these two particular parts. It should be noted here that all the stresses were below the 12,000 psi value of the proportional limit for the material, which restricts both theory and experiment to the elastic range.

CHAPTER VII

CONCLUSIONS AND RECOMMENDATIONS

Since the experimental part of this thesis was restricted to two indeterminate structures, it would be difficult to conclude that the solution advanced here would apply equally well to any other part. It is thus necessary to restrict this solution to parts of the same general design as the two used in this thesis until further experimental work is performed.

It was noted in the theoretical solution of deflections and later verified by experiment that the deflection under a given clamping load was greater for Part I than it was for Part II. This was due to the larger projecting arms on Part II which substantially increased the stiffness of this part (see pages 22 and 29). It can be seen from this that the projecting arms should be made as small as possible in order to make the part more flexible.

In the light of these observations the following recommendations are made:

1. Additional tests should be made on parts of several different shapes to check the correctness of the equations presented in this thesis as to their general application. The cross sections used in these additional experiments could be different than the ones used in this report and additional equations could be derived using the same approach as presented.

2. Emphasis should be placed on the proper design of any clamped part so it will be as flexible as possible in order to decrease the maximum clamping stresses.

BIBLIOGRAPHY

1. Perry, C. C. and H. R. Lissner, The Strain Gauge Primer. New York: McGraw-Hill Book Company, 1955.